Atmos. Chem. Phys. Discuss., doi:10.5194/acp-2017-150, 2017
Manuscript under review for journal Atmos. Chem. Phys.
Discussion started: 26 April 2017

Atmospheric Chemistry and Physics Discussions

Sources of Submicrometre Particles Near a Major International Airport

Mauro Masiol[1,2], Roy M. Harrison[1*†], Tuan V. Vu[1], David C.S. Beddows[1]

[1] Division of Environmental Health and Risk Management School of Geography, Earth and Environmental Sciences University of Birmingham Edgbaston, Birmingham B15 2TT United Kingdom

[2] Center for Air Resources Engineering and Science, Clarkson University, Potsdam, NY 13699, United States

[*] To whom correspondence should be addressed.
Tele: +44 121 414 3494; Fax: +44 121 414 3709; Email: r.m.harrison@bham.ac.uk

[†]Also at: Department of Environmental Sciences / Center of Excellence in Environmental Studies, King Abdulaziz University, PO Box 80203, Jeddah, 21589, Saudi Arabia

Atmos. Chem. Phys. Discuss., doi:10.5194/acp-2017-150, 2017
Manuscript under review for journal Atmos. Chem. Phys.
Discussion started: 26 April 2017

Atmospheric Chemistry and Physics Discussions

ABSTRACT

Major airports are often located within or close to large cities; their impacts on the deterioration of air quality at ground level are amply recognised. The international airport of Heathrow is a major source of nitrogen oxides in the Greater London area, but its contribution to the levels of submicrometre particles is unknown, and is the objective of this study. Two sampling campaigns were carried out during warm and cold seasons at a site close to the airfield (1.2 km). Size spectra were largely dominated by ultrafine particles: nucleation particles (<30 nm) were found to be ~10 times higher than those commonly measured in urban background environments of London. A set of chemometric tools was used to discern the pollution arising from aircraft operations and those from other sources within the city or from the traffic generated by the airport. Five clusters and 6 factors were identified by applying *k*-means cluster analysis and positive matrix factorization (PMF) respectively to particle number size distributions; their interpretation was based on their modal structures, wind directionality, diurnal patterns, road and airport traffic volumes and on the relationship with weather and other air pollutants. Airport emissions, fresh and aged road traffic, urban accumulation mode and two secondary sources were then identified and apportioned. The comparison of cluster and PMF analyses allowed extraction of further information. The analysis of a strong regional nucleation event was also performed to detect its effect upon concentrations. The fingerprint of Heathrow has a characteristic modal structure peaking at <20 nm and accounts for 30-35% of total particles in both the seasons. Other main contributors are fresh (24-36%) and aged (16-21%) road traffic emissions and urban accumulation from London (around 10%). Secondary sources accounted for less than 6% in number concentrations but for more than 50% in volume concentration. In 2016, the UK government provisionally approved the construction of a third runway; therefore the direct and indirect impact of Heathrow on local air quality is expected to increase unless mitigation strategies are applied successfully.

Keywords: Airport; black carbon; size distributions; source apportionment; ultrafine particles

Atmos. Chem. Phys. Discuss., doi:10.5194/acp-2017-150, 2017
Manuscript under review for journal Atmos. Chem. Phys.
Discussion started: 26 April 2017

Atmospheric Chemistry and Physics Discussions

1. INTRODUCTION

Emerging markets, developing economies and globalisation are driving a fast and continuing growth of civil aviation, which is expected to continue in the next decade (Lee et al., 2009). As a consequence, the aircraft and road traffic at airports is also increasing, but the information available on the impact of airport emissions upon air quality at ground level is still inadequate (Webb et al., 2008; Masiol and Harrison, 2014). The quantification of airport impacts on local air quality is complicated by the complexity of multiple mobile and static emission sources, with many airports being located near to major cities, highways or industrial plants. Under this scenario, the development of successful strategies for emission mitigation and the implementation of measures for air quality control to meet regulatory standards require an exhaustive quantification of the contribution of airport emissions to the total air pollution load.

London Heathrow (LHR) is one of the world's busiest international airports: it is ranked 1st in Europe for total passenger traffic (ACI, 2016). Its role in driving the economic affluence and vitality of the Southern UK is indisputable: it accommodates more than 1250 flights every day and serves a total of 72.3 million passengers year^{-1}. LHR is composed of 5 terminals and 2 runways: northern (3.9 km-long) and southern (3.7 km). Currently, runways operate near their maximum capacity, with a consequent increase in the potential for delays when flights are disrupted. Since 2007, the proposal for expanding LHR with a 3rd runway and a 6th terminal has been intensely debated in UK. The main reasons supporting its expansion are: (i) the expected increase of resilience to disruption caused by congested flight traffic; (ii) the improvement of its connectivity with a profitable network of both direct long haul air routes and national flight connections; (iii) the potential to directly enhance the economic growth of the London area. On the contrary, opposition to LHR expansion highlights the potential increases in air pollution and noise, the community destruction and argues in favour of alternative options with fewer local impacts, such as the improvement of other airports in the southern UK or the building of a new airport in the Thames

Atmos. Chem. Phys. Discuss., doi:10.5194/acp-2017-150, 2017
Manuscript under review for journal Atmos. Chem. Phys.
Discussion started: 26 April 2017

Estuary (East of London). Despite this, in 2016 the UK government provisionally approved the construction of a third runway.

Greater London is one of the few UK locations not fully achieving the EU and national air quality standards: in 2015 nitrogen dioxide breached the hourly and annual limit values for health, while ozone exceeded the long-term objective (DEFRA, 2016). On the other hand, the mass concentration of particulate matter (PM), which is the standard current metric for measuring and controlling the exposure to airborne particles, was fully met for both PM_{10} and $PM_{2.5}$. However, it has been widely demonstrated that even PM mass concentrations below guidelines and standards set by legislatures or international organizations may increase acute and chronic effects and mortality (e.g., Shi et al., 2015). In this situation, the use of mass concentration as a sole metric for measuring the levels or airborne particles has the disadvantage of taking greatest account of accumulation and coarse mode particles, which account for most of the mass. Consequently, the impact of the finest particles is not accounted for directly. This issue raises serious questions for the air quality standards: biological evidence associates the exposure to ultrafine particles (UFPs, <100 nm) with adverse effects upon human health (e.g., Knibbs et al., 2011; Strak et al., 2012; Ostro et al., 2015; Lanzinger et al., 2016). At the current time, there is still limited knowledge of what specific characteristic or association of characteristics may dominate the particle toxicity, and the consequent health outcomes (Atkinson et al., 2010; Strak et al., 2012, Vu et al., 2015a); nevertheless it is well recognised that UFPs can reach the deepest regions of the lung (Salma et al., 2015) and may have orders of magnitude higher surface area to mass ratios compared to larger particles. They offer more surface for the absorption of volatile and semi-volatile species (Kelly and Fussell, 2012; Strak et al., 2012). However, there are currently no ambient air quality standards or guidelines to drive the regulation of UPF.

The goal of this study was to investigate the impacts of a major airport (LHR) serving a megacity (London) upon the levels of submicrometre particles and equivalent black carbon (eBC) and to

apportion those impacts to aircraft, road traffic and other sources typical of large cities with airports. This task was performed by collecting air quality data at a site downwind of LHR and by applying a series of chemometric tools. The potential sources of submicron particle number concentrations (PNC) are investigated by applying two source apportionment methods: cluster analysis and positive matrix factorisation (PMF). Thus, the origin of the airport plumes was spatially assessed by matching results with local meteorological data, air mass movements, levels of common air pollutants, $PM_{2.5}$ mass concentration and its chemical speciation as an indicators of source location and formation mechanisms. Finally, the disaggregated source profiles are used to trace the factors affecting the pollutant levels, such as atmospheric dispersion and processing of aircraft emissions as well as of road traffic.

This study was carried out under the Marie Skłodowska-Curie project CHEERS (Chemical and Physical Properties and Source Apportionment of Airport Emissions in the context of European Air Quality Directives, call: FP7-PEOPLE-2012-IEF, project no. 328542).

2. MATERIALS AND METHODS

2.1 Study Area and Dates

The summer (warm season) campaign took place from 13 August to 12 September 2014 and the winter (cold season) campaign from 19 December 2014 to 20 January 2015. The Greater London area hosts more than 8.5 million inhabitants and LHR is located west of London (Figure 1). Consequently, air quality in the surroundings of the airport may be affected by the advection of air masses from the city, with the associated high levels of pollutants emitted from traffic, energy demand for domestic heating and local industries. Airport activities may also contribute to air pollution advected to the city when LHR is upwind, with consequent potential impacts upon public health. In addition, as LHR attracts a large number of passengers and workers, the emissions from large volumes of road traffic generated by the airport and the nearby M4 and M25 motorways are

difficult to discriminate from non-airport-related road traffic. Due to this complex scenario, the contribution of LHR is difficult to differentiate from the urban background pollution, as already reported by previous modelling and experimental studies (Farias and ApSimon, 2006; Masiol and Harrison, 2015).

Various studies have attempted to quantify the effect of LHR upon air quality, mainly focusing on the nitrogen oxides (NO_x=NO+NO_2), which are well-known tracers for aircraft engine exhausts (e.g., Herndon et al., 2008; Masiol and Harrison, 2014 and references therein), but also arise from other combustion sources. For example, Carslaw et al. (2006) estimated that airport operations in 2001/4 accounted for ~27% of the annual mean NO_x and NO_2 at the airfield boundary and less than 15% (<10 µg m^{-3}) at background locations 2-3 km downwind of the airport. Similar results were found for the 2008/9 period using model evaluation (AEA, 2010) and for the 2005/12 period using experimental data analysis (Masiol and Harrison, 2015). This latter study also reported that PM mass concentrations at eight sites all around LHR were always well below the EU and UK limit.

2.2 Site Description

Two intensive sampling campaigns (each 1 month-long) were carried out during warm (August-September 2014) and cold (December 2014-January 2015) periods at Harlington (Figure 1). Data from the site are quality assured as part of the UK Automatic Urban and Rural Network under the auspices of the UK Department for Environment, Food and Rural Affairs (DEFRA; http://uk-air.defra.gov.uk/) and the site was selected as well located to sample the plumes from the airport emissions. The site lies 1.2 km N of the northern runway and is located inside a playground, close to a secondary road and near the village of Harlington. This is the location selected for the construction of the 3rd runway. The site is categorised as “urban industrial” by DEFRA and it is therefore more indicative of community exposure rather than direct fresh aircraft emissions. Consequently, it is a good point to quantify the particles generated by the airport after a relatively

short ageing and dispersion in the atmosphere, and is more indicative of the fingerprint of aircraft emissions affecting communities than data collected alongside the runway or in the airport apron areas. In addition, previous studies have reported that the site is strongly affected by the plume from the airport (Carslaw et al., 2006; Masiol and Harrison, 2015). Prevailing winds from the 3rd and 4th quadrants are recorded in both summer and winter (Figure SI1): under such circulation regimes, Harlington lies just downwind of LHR. However, the site is also affected by pollutants arising from the large volumes of road traffic generated by the airport: Tunnel Rd., the main access to LHR from the M4 motorway lies 800 m west, as well as the nearby M4 (640 m north) and M25 (~3.5 km east) motorways, major roads (Bath Rd, part of A4, passes 900 m south; A30 lies 2.8 km SE). The village of Harlington (~400 m west) and the conurbation of London are other potential external sources.

2.3 Instrumentation Suite

Ultrafine particle counts and their size distributions from 14.3 to 673.2 nm were measured at 5 min time resolution using a SMPS (scanning mobility particle sizer spectrometer) comprising a electrostatic classifier TSI 3080 with a long differential mobility analyser (TSI 3081) and a CPC (condensation particle counter, TSI 3775) based on condensation of *n*-butyl alcohol (Fisher Scientific, ACS). The SMPS operated at a sheath air to aerosol flow ratio of 10:1 (sheath and sample air flow rates were 3.0 and 0.3 L min^{-1} respectively, voltage 10-9591 V; density 1.2 g/cc; scan time 120 s, retrace 15 s; number of scan 2) while the CPC operated at low flow rate (0.3 L min^{-1}). The use of 5 min resolved spectra has already been used successfully for source apportionment purposes at an airport (Masiol et al., 2016).

eBC was also measured at 5 min resolution using a 7-wavelength aethalometer (Magee Scientific AE31). The aethalometer operated with an inlet cut-off head to collect PM with aerodynamic

Atmos. Chem. Phys. Discuss., doi:10.5194/acp-2017-150, 2017
Manuscript under review for journal Atmos. Chem. Phys.
Discussion started: 26 April 2017

185 diameter of <2.5 μm ($PM_{2.5}$). eBC was derived from the absorbance at 880 nm wavelength (Petzold
186 et al., 2013).
187
188 Instruments were installed into a plastic/metal case designed for sampling purposes: (i) air inlets
189 were ~1.8 m over the ground and were composed of conductive materials to avoid particle losses
190 and sampling artefacts; (ii) the case was cooled by fans in summer and was warmed by an electrical
191 tubular heater in winter for maintaining an indoor air temperature within an acceptable range for
192 running the equipment (temperature inside the case was recorded and periodically checked); (iii)
193 instruments were isolated from vibration using rubber pads and foam foils. Devices were fully
194 serviced, calibrated by authorised companies and underwent internal cross-calibrations with other
195 similar instruments under lab conditions. Moreover, frequent periodic checks, maintenance of
196 instruments and cleaning of inlets was performed throughout the sampling campaign.
197
198 Classical air pollutants (NO, NO_2, NO_x, O_3, PM_{10}, $PM_{2.5}$) were measured at Harlington with 1 h
199 time resolution. Gaseous species were analysed using automatic instruments according to European
200 standards and National protocols: EN 14211:2012 for nitrogen oxides and EN 14625:2012 for
201 ozone. PM_{10} and $PM_{2.5}$ were analysed using tapered element oscillating microbalance and filter
202 dynamics measurement system (TEOM-FDMS) to provide measurements accounting for volatile
203 (VPM_{10}, $VPM_{2.5}$) and non-volatile ($NVPM_{10}$, $NVPM_{2.5}$) fractions. Quality assurance and quality
204 control procedures followed the standards applied for the Automatic Urban and Rural Network
205 (AURN) and the London Air Quality Network (LAQN). Instruments were routinely calibrated, and
206 every six months were fully serviced and underwent intercalibration audits.
207
208 Weather data were measured hourly by the Met Office at LHR; met data include wind direction and
209 speed, atmospheric pressure, air temperature, relative humidity (RH), visibility, rain and solar
210 irradiance.

Atmos. Chem. Phys. Discuss., doi:10.5194/acp-2017-150, 2017
Manuscript under review for journal Atmos. Chem. Phys.
Discussion started: 26 April 2017

Atmospheric Chemistry and Physics Discussions

During the two campaigns, 24-h $PM_{2.5}$ samples were also collected on quartz filters using a high volume air sampler (TE-6070, Tisch Environmental, Inc.) and analysed for the daily concentrations of major $PM_{2.5}$ components: organic carbon (OC) and elemental carbon (EC) by thermo-optical analysis (EUSAAR_2 protocol) and major inorganic ions (Na^+, K^+, ammonium, nitrate, sulphate, oxalate) by ion chromatography. Analytical methods are reported in detail in Yin et al. (2010). The results of the chemical speciation of $PM_{2.5}$ are presented in a companion paper (in preparation) and are used in this study only to assist the interpretation of PMF results.

2.4 Data Handling and Chemometric Approaches

Data were analysed using R version 3.3.1 (R Core Team, 2015) and a series of supplementary packages, including 'Openair' (Carslaw and Ropkins, 2012). Preliminary data handling and clean-up were carried out to check the robustness of the dataset, detect anomalous records and to delete extreme outliers. SMPS data with unreliable behaviour or instrument errors were completely deleted. All remaining data are used for descriptive statistics, but data greater than the 99.5th percentile were further removed for explorative, cluster and PMF analyses. Missing data for other variables were linearly interpolated between the nearest values of the time series.

The particle number size distributions (PNSDs) were firstly grouped by applying a *k*-means cluster analysis. The full method is exhaustively discussed in Beddows et al. (2009; 2014) and aims to assemble single spectra into *k* clusters. The clustering groups observations with spectra similar to their cluster centroids (means), i.e. observations that are likely generated by the same set of formation processes or emission sources. The optimum number of clusters (*k*) was determined by an optimisation algorithm based on the spectral shapes (Beddows et al., 2009). The choice to apply *k*-mean clustering method was based on several reasons: (i) Salimi et al. (2014) reported that *k*-means is the best performing clustering among others methods tested on PNSD data; (ii) *k*-means is a well-

established method which has been largely applied over a number of different sites (e.g., Dall'Osto et al., 2012; Wegner et al., 2012; Beddows et al., 2014; Brines et al., 2014; 2015); and (iii) the method was previously applied successfully to airport data (Masiol et al., 2016).

PMF analysis was performed by applying the USEPA PMF5 model. Details of the PMF model are reported elsewhere (Paatero and Tapper, 1994; Paatero, 1997; USEPA, 2014), while the best practice and standards are extensively reviewed in several papers (e.g., Reff et al., 2007; Belis et al., 2014; Brown et al., 2015; Hopke, 2016). SMPS data at 5 min resolution were used as the PMF input matrix. Uncertainties associated with SMPS data were estimated according to the empirical method proposed by Ogulei et al. (2007). Uncertainty for the total variable (total particle number concentration, PNC) was set at 300% of the PNC concentration and also marked as "weak" to avoid it driving the profiles.

A series of additional tools were used to analyse the raw data, link source apportionment results to other variables, such as local atmospheric circulation and regional/transboundary transport of air masses. Briefly, polar plots aim to map pollutant average concentrations by wind speed and direction as continuous surfaces (Carslaw et al., 2006), while polar annuli plot by wind direction and hours of the day. The potential locations of distant sources were assessed using back-trajectory analysis and a concentration weighted trajectory (CWT) model (Stohl, 1998). Back-trajectories were computed with the HYSPLIT4 model (Stein et al., 2015; Rolph, 2016) using NCEP/NCAR reanalysis gridded meteorological data. Set-up: -96 h with a starting height of 500 m a.g.l. CWT is a method of weighting trajectories with associated concentrations to detect the most probable source areas of long-range transports of pollutants; it has been used and reviewed in a number of prior studies (e.g., Stohl, 1996; Lupu and Maenhaut, 2002; Squizzato and Masiol, 2015).

Atmos. Chem. Phys. Discuss., doi:10.5194/acp-2017-150, 2017
Manuscript under review for journal Atmos. Chem. Phys.
Discussion started: 26 April 2017

3. RESULTS AND DISCUSSION

3.1 Overview of Data

The wind roses during the two sampling periods are provided in Figure 1. Descriptive statistics of all collected variables are aggregated as boxplots in Figure 2a. Some additional variables are also computed to help the interpretation of results. The NO_2/NO_x ratio is indicative of the partitioning of nitrogen oxides, while the levels of oxidants ($OX=O_3+NO_2$, expressed in ppbv) can be used to roughly assess the oxidative potential in the atmosphere (Kley et al., 1999; Clapp and Jenkin, 2001). These two new variables are useful in investigating the atmospheric chemistry behind the NO-NO_2-O_3 system. Delta-C (the difference between absorbance at 378 and 880 nm, also called UVPM) was also computed. This variable was largely used as a proxy to estimate the fraction of carbonaceous material emitted by biomass burning (e.g., Sandradewi et al., 2008; Wang et al., 2011). However, Delta-C results should be used with caution: Harrison et al. (2013) showed that there are probably other UV absorbing contributors than wood-smoke to the aethalometer signal. This way, Delta-C is used here only for qualitative purposes.

PNSDs were initially split into 3 ranges: nucleation (14-30 nm), Aitken nuclei (30- 100 nm) and accumulation (>100 nm). On average the total PNC during the warm season was $1.9 \cdot 10^4$ particles cm^{-3}, of which 1.1×10^4, 6.4×10^3 and 1.5×10^3 particles cm^{-3} were classified as nucleation, Aitken and accumulation ranges, respectively. During the cold season, the total average PNC was 2.2×10^4 particles cm^{-3}, composed of 1.4×10^4, 6.3×10^3 and 1.4×10^3 particles cm^{-3} as nucleation, Aitken and accumulation ranges, respectively. Concentrations lie between those of London, Marylebone Road (kerbside) and London, North Kensington (background), and nucleation particles were ~10 times higher than the annual average measured in North Kensington as reported by Vu et al. (2016), while Aitken particles were 1.9 times higher. It is therefore evident that the main difference lies in the concentration of the finest size ranges: in both seasons, spectra were dominated by UFP (D_p<100 nm) particles (~92% of total PNC), which only accounted for ~12% of total particle

289 volume concentration (PVC, computed by approximation to spherical particles). On the other hand,
290 accumulation mode particles accounted for ~8% of PNC and ~88% of PVC volume.
291
292 The high levels of total PNC are not surprising. Several studies have reported large increases in
293 PNC near airports. For example, Hsu et al. (2013) and Stafoggia et al. (2016) detected substantial
294 increases of PNC values at the airports of Los Angeles (CA, USA) and Rome Ciampino (Italy),
295 respectively, in the few minutes after take-offs, especially downwind, while landings made only a
296 modest contribution to ground-level PNC observations. Hsu et al. (2014) observed that departures
297 and arrivals on a major runway of Green International Airport (Warwick, RI, USA) had a
298 significant influence on UFP concentrations in a neighborhood proximate to the end of the runway.
299 In a study carried out at the Los Angeles international airport (CA, USA), Hudda et al. (2014)
300 concluded that emissions from the airport increase PNC by 4- to 5-fold at 8–10 km downwind of
301 the airfield, while Shirmohammadi et al. (2017) reported that the daily contributions of the airport
302 to PNC were approximately 11 times greater than those from three surrounding freeways. Hudda et
303 al. (2016) reported that average PNC were 2- and 1.33-fold higher at sites 4 and 7.3 km from the
304 Boston (MA, USA) airport when winds were from the direction of the airfield compared to other
305 directions. The site used in this study is even closer to the airfield (1.2 km) and is also affected by
306 strong non-airport sources, such as road traffic emissions due to the presence of two motorways and
307 several busy roads (frequently congested).
308
309 During the warm season, the average concentrations for other pollutants followed the order (in μg
310 m^{-3}): NO_x (49)> O_3 (31)> NO_2 (31)> PM_{10} (20)> $NVPM_{10}$ (16)> $PM_{2.5}$ (14)> NO (12)> $NVPM_{2.5}$
311 (11)> VPM_{10} (4)> $VPM_{2.5}$ (3.2)> eBC (2.4)> Delta-C (<0.1). The average concentrations during the
312 cold season were: NO_x (83)> NO_2 (38)> O_3 (34)> NO (29)> PM_{10} (18)> $NVPM_{10}$ (14)> $PM_{2.5}$
313 (13)> $NVPM_{2.5}$ (9.8)> VPM_{10} (4.3)> $VPM_{2.5}$ (3.4)> eBC (2.1)> Delta-C (0.2). These values are
314 similar to the average concentrations for common air pollutants measured in the vicinity of LHR

315 reported by Masiol and Harrison (2015) over an 8 year period (2005-2012). Consequently, despite
316 the intensive sampling campaign carried out in this study, results may be considered representative
317 of the average levels of air pollution recorded at Harlington.
318 Since the data were generally not distributed normally, the nonparametric Kruskal-Wallis one-way
319 analysis of variance was used to test the difference of concentrations over the two periods: almost
320 all variables are different at the 0.05 significance level, except NO, NO_x and O_3. This result
321 indicates a seasonal effect upon air quality in the LHR area and suggests investigating the sources
322 over the two periods separately.
323
324 The PNSDs are shown in Figure 3. Spectra are categorised by time of day (7am-7pm and 7pm- 7am
325 local time). In addition, the particle volume size distributions (PVSDs) are also provided. Results
326 show that in both seasons the nocturnal data are shifted toward coarser modes with respect to the
327 diurnal mean PNSD, while the modal structure of PNVDs is almost constant throughout the day.
328
329 The diurnal cycles of most important variables are shown in Figure 2b. Generally, diurnal cycles
330 derive from the interplay of emissions, dispersion and atmospheric chemical processes.
331 Consequently, they need to be investigated along with patterns for airport and motorway traffic
332 (Figure 2b and Figure SI2, respectively), and as polar annuli (Figures SI3 and SI4) and polar plots
333 (Figures SI5 and SI5), which give preliminary insights upon the origin and spatial location of most
334 probable emission sources. Airport traffic undergoes to some restrictions to limit noise community
335 disturbance: flights are generally constant from 6 am to 8 pm and are kept at minimum overnight,
336 with no departures normally scheduled between 11 pm and 6 am (Figure 2b). Road traffic is more
337 difficult to define. Data for M4 and M25 motorways are provided by the UK Department for
338 Transport: data for the M4 motorway show typical morning (7-8 am) and evening (5-6 pm) peaks
339 due to rush hours, but this pattern is not well-resolved for the M25 (Figure SI2). In addition, despite
340 it being likely that traffic on minor and local roads also follows patterns dominated by rush hours,

traffic generated by the airport is more difficult to characterise, with Tunnel Rd. and other busy roads serving LHR being frequently congested.

Nucleation particles are likely associated with aircraft movements: the daily pattern shows almost constant concentrations between 7 am and 10 pm, while levels drop to near-zero overnight; the maximum average concentrations are recorded for winds blowing from the SW quadrant, i.e. the airfield and, in particular, the location of the main LHR terminals. As a consequence of the dominance of nucleation particles over size spectra, also total PNC follows this pattern. On the contrary, accumulation particles appear to be associated with road traffic, i.e. daily cycles show typical rush hour peaks and increases for winds blowing from northern sectors. Aitken nuclei exhibit an intermediate behaviour between nucleation and accumulation particles: two different patterns can be found, which are more consistent with road traffic in summer and with aircraft traffic in winter.

Nitrogen oxides are key air pollutants for this study: (i) NO_2 levels do not fully fulfil the air quality assessment Limit Values for health (1 h and annual mean) in the Greater London urban area (DEFRA, 2016); (ii) they can be good tracers for airport emissions, since NO_2 is the main species of nitrogen oxides emitted by turbofan engines at idle, while NO is the dominant species at higher thrust (Wormhoudt et al., 2007; Masiol and Harrison, 2014); (iii) they are also emitted from road traffic mainly as NO, although recent non-attainments of NO_2 standards in Europe have been linked to the growing proportion of diesel-powered vehicles, which have higher primary (direct) emissions of NO_2 (Carslaw et al., 2007; Grice et al., 2009; Anttila et al., 2011; Cyrys et al., 2012). In addition, nitrogen oxides and atmospheric oxidants are strongly linked by a series of chemical reactions which are responsible for their partitioning between NO and NO_2 (Finlayson-Pitts and Pitts, 2000; Seinfeld and Pandis, 2006). To date, NO_x has been thoroughly investigated at LHR (Carslaw et al., 2006; Masiol and Harrison, 2015): it was estimated that the upper limit contribution of LHR

activities to NO_2 at Harlington during the 2001-2012 period was ~15-17%, while that for NO was ~10%. In this study, nitrogen dioxide exhibits two typical rush hour peaks, as previously also observed at the London, North Kensington urban background site (Bigi and Harrison, 2010), and its concentration increases for winds blowing from all quadrants, suggesting a mix of different sources, including airport, road traffic and other combustion emissions. Nitric oxide only shows the morning rush hour peak and northern directionality (toward the M4 motorway) in summer, while in winter it lacks any significant pattern. The difference between the patterns of NO and NO_2 during the two periods is also confirmed by the NO_2/NO_x ratio, which shows a morning rush hour minimum in summer as a consequence of fresh NO emissions, while it is less variable in winter (Figure 2b).

In 2015, ozone met the EU target value, but not the long-term objective in the Greater London area (DEFRA, 2016). In this study, it does not present any wind directionality and exhibits an evident daily peak in the mid-afternoon, i.e. when the photochemical activity is enhanced by the higher solar irradiation and the boundary layer depth is greatest, while a second peak in the early morning corresponds to a minimum in NO (Figure 2b).

Despite some studies indicating that airports are strong sources of black carbon (Dodson et al., 2009), other studies report no strong relationships with the flight activity (Masiol et al., 2016; Hsu et al.,2016). Similarly to NO_2, aethalometer data also shows typical patterns of road traffic-influenced sites for all wavelengths, with two daily peaks corresponding to the hours with higher traffic. However, Delta-C does not present any evident pattern. eBC shows increased concentrations when winds blow from northern sectors (plus SE in winter); which excludes airport activities as being a dominant source in the study area.

Particulate matter (PM_{10} and $PM_{2.5}$) has very weak diurnal patterns. Its wind directionality shows evident increases for northerly winds. It is therefore evident that PM mass concentrations are

393 dominated by non-airport sources, i.e. regional secondary pollutants, traffic from the nearby M4 or
394 background pollution from London. $PM_{2.5}$ concentrations normally do not exceed the Limit Values
395 in the Greater London area (DEFRA, 2016).
396
397 **3.2 *k*-means Cluster Analysis**
398 The clustering algorithm extracted 5 clusters for both periods. The number of clusters was selected
399 according to the optimisation algorithm, i.e. local maxima in the Dunn indices and silhouette
400 (Beddows et al., 2009). The extraction of 5 clusters represents a good compromise for the
401 interpretation of spectral observations. Hussein et al. (2014) reported that is not prudent to describe
402 the spectra with few clusters (2-4), which are not sufficient to explain variations and detailed
403 differences in the PNSD observed in the urban atmosphere. On the other hand, they also reported
404 that extracting too many (>10) clusters may make the aerosol source attribution more challenging.
405
406 The cluster centroids (mean spectra of each cluster), the 10th, 25th, 75th and 90th percentile, the
407 hourly counts patterns and resulting wind roses are shown in Figure 4 and 5 for the warm and cold
408 season campaigns, respectively. Despite extracted clusters exhibiting significantly different modal
409 structures for PNC, no differences can be observed for the particle volume size spectra, which all
410 show a unimodal peak at approx. 200-300 nm.
411
412 *3.2.1 Warm season*
413 During the warm season, 20% of total clustered observations were grouped in *cluster 1*. It presents a
414 sharp peak for nucleation particles which extends below the SMPS detection limit (14 nm), a large
415 increase in frequency during the afternoon hours (noon to 7pm) and its wind rose shows that this
416 spectrum shape mostly occurs when the prevailing wind blows from SW. Aircraft are known to
417 emit particles in the nucleation range (e.g. Mazaheri et al., 2009;2013; Masiol and Harrison, 2014;
418 and references therein; Lobo et al., 2015) and the wind rose is also compatible with an origin from

419 the airfield and the main LHR terminals. However, a similar PNSD profile and a similar daily
420 pattern was also reported in North Kensington (London background) by Vu et al. (2016) and was
421 associated with nucleation events. Its interpretation can thus be associated either with airport
422 activities or photochemical nucleation.
423
424 *Clusters 2 and 3* account for 19% and 23% of observations, respectively. While cluster 2 shows a
425 main peak in number concentrations at 30-40 nm, cluster 3 is bimodal (14 and 60-70 nm). Both
426 clusters exhibit similar hourly count profiles with most of the counts occurring overnight. This
427 pattern is largely attributable to the dynamics of the mixing layer, since the diurnal cycles are the
428 mirror image of the ambient air temperature (Figure 2b). Because of this, both clusters are strongly
429 affected by the reduced height of the mixing layer occurring overnight. In addition, the role of the
430 nighttime nitrate formation through condensation of NH_4NO_3 and the heterogeneous reactions of
431 N_2O_5 and NO_3 on pre-existing particles cannot be ignored (Seinfeld and Pandis, 2006; Bertram and
432 Thornton, 2009; Brown and Stutz, 2012). However, such clusters occur under different wind
433 regimes, as the wind roses indicate two different potential source locations: cluster 2 shows a
434 possible origin from W sectors, while cluster 3 indicates the NE. From this we can infer that cluster
435 2 likely represents PNSD shaped by: (i) regional aerosols, since the wind directionality suggests an
436 origin from regions west of London, an area with a lower density of anthropogenic sources, and (ii)
437 emissions from the M25 motorway and Tunnel Road, i.e. it can be influenced by aged road traffic
438 emissions. This latter interpretation is also supported by the presence of a peak in the hourly counts
439 corresponding to the morning rush hours. On the other hand, cluster 3 likely represents the particle
440 size spectra mainly shaped by primary and secondary aerosols advected from the most urbanised
441 areas, i.e. it can be likely associated to the urban background of London.
442
443 The last two clusters are probably associated with road traffic: vehicle exhaust emissions peak in
444 the Aitken and accumulation modes with the size ranging from 20 nm to 500 nm (Vu et al., 2015b,

and references therein). *Cluster 5* accounts for 14% of observations and reveals a unimodal structure peaking at 25 nm. The hourly count pattern exhibits two maxima (6-8 am and 4-8 pm) related to morning and evening rush hours. The wind rose shows that observations in this cluster mostly occur when air masses blow from westerly sectors, which are compatible with the location of motorways and Tunnel Rd, the main roadway linking LHR to the M4 motorway. In addition, it can be noted that the wind rose exhibits high percentages of high speed winds from W. This pattern is compatible with fresh road traffic emissions.

Cluster 4 represents 25% of total observations. It peaks at smaller particle sizes, but also shows a wide hump at 50-150 nm. It is recognised that road traffic contributes to a large range (30-200 nm) of PNSD in the urban atmosphere (e.g., Yue et al., 2008; Costabile et al., 2009; Harrison et al., 2011), which is compatible with this cluster spectrum. In addition, the hour count profile presents a huge maximum during daytime with possibly 3 maxima (morning and evening rush hours plus mid-afternoon); this pattern is the mirror image of those for clusters 2 and 3. The directional analysis shows increased levels when air masses move from the sectors more affected by traffic: London (NE), M4 (N) and M25 (W) motorways and Tunnel Rd (W). It may represent the typical spectra recorded during daytime and can be associated with aged anthropogenic emissions, mostly due to road traffic.

3.2.2 Cold season

Unfortunately, the atmospheric circulation during the cold season mostly experienced winds blowing from the SW quadrant, while the NE sectors were poorly represented. As a consequence, the limited extent of the wind directionality analysis may blur the interpretation of results. In addition, the limited number of observations for air pollution advected from the Greater London area may have affected the detection of the urban background.

471 *Clusters 1 and 5* account for 24% and 17% of total observations, respectively. They occur under
472 comparable wind regimes (from SW) and timing (increased counts during daytime). While the
473 diurnal pattern of cluster 1 has the same shape as the LHR aircraft movement profiles (Figure 2),
474 cluster 5 is more comparable with cluster 1 for the warm season (maximum in the early afternoon).
475 However, their spectra are quite different: cluster 1 has a main mode at 20-25 nm, while cluster 5
476 peaks at 15 nm. Based on the prevailing wind directionality, they can both be linked to airport
477 activities. A close analysis of wind roses reveals that cluster 5 occurs at significantly higher wind
478 speed regimes than cluster 1 (Mann-Whitney-Wilcoxon test at 0.05 significance level), i.e. average
479 wind speeds of 8.3 and 5.9 m s^{-1}, respectively. A possible interpretation is that cluster 5 represents
480 fresher airport emissions (this may also explain the high similarity with the cluster 1 for the warm
481 season), while cluster 1 depicts the airport emissions which have undergone more aging. The aging
482 of freshly emitted particles in the atmosphere may involve condensation, evaporation and
483 agglomeration processes and has been demonstrated to be a major mechanism in altering aerosol
484 PNSD (e.g., Shi et al., 1999; Kim et al., 2004; Zhang et al., 2005; Zhou et al., 2005; Zhang et al.,
485 2011; Harrison et al., 2016); this effect was also observed for particles emitted by road traffic in
486 London (Dall'Osto et al., 2011). Another possible interpretation is that one cluster could represent
487 the PNSD mainly influenced by aircraft engine emissions, while the other is related to other on-
488 airport sources, e.g., airport ground service equipment, emissions from auxiliary power units (small
489 on-board gas-turbine engines) or ground power units provided by the airport. However, this latter
490 interpretation is less probable, since the spatial extent and temporal pattern of these two sources is
491 the same (airfield) and, thus, they are expected to be much better mixed.
492
493 *Cluster 2* (16% of observations) extends over a wide size range (20 to 150 nm) and presents a daily
494 pattern likely attributable to the dynamics of the mixing layer (the pattern is the mirror image of the
495 ambient air temperature). In winter, there is a stronger effect of the mixing layer dynamics on the
496 air quality due to the presence of more frequent low level thermal inversions which may build up

497 the pollutants at ground-level especially overnight. Consequently, this cluster cannot be linked to
498 any specific primary anthropogenic source in the study area, and is likely representative of spectra
499 mostly shaped by the drop of the mixing layer height and the formation of secondary aerosols.
500
501 *Cluster 3* accounts for 20% of data during the cold season. The size spectrum, the wind rose and,
502 partially, the hourly count profile well relates to cluster 5 for the warm season (attributed to fresh
503 road traffic emissions). However, the diurnal pattern also presents a high number of counts at 3-5
504 am, i.e. not compatible with rush hours. Wood smoke is recognised to peak around 100 nm (e.g.,
505 Chandrasekaran et al., 2013; Vu et al., 2015b). A possible interpretation is that observations
506 included in this cluster may represent PNSDs dominated by both traffic but influenced by domestic
507 biomass combustion.
508
509 *Cluster 4* (22%) peaks at 17 nm and also shows a wide hump at 50-150 nm. Its diurnal pattern
510 shows a marked maximum occurring on the afternoon and is mostly represented under westerly
511 winds regimes. Considering the differences between the two campaigns, it has similar
512 characteristics to cluster 4 for the warm season. Thus, it can be interpreted as typical of spectra
513 recorded during daytime and associated with the aging of anthropogenic emissions, mostly due to
514 road traffic.
515
516 **3.3 PMF Analysis**
517 The best PMF solutions were identified: (i) by investigating solutions between 3 and 10 factors; (ii)
518 by considering the minimization of the function *Q* with respect to the expected (theoretical) value
519 and its stability over multiple (n=100) runs, (iii) by obtaining low values for the sum of the squares
520 of the differences in scaled residuals for each base run pair by species; (iv) by minimizing the
521 number of absolute scaled residuals over ±3 and by keeping them symmetrically distributed; (v) by
522 keeping the result uncertainties calculated by bootstrap (BS, n=200) and displacement (DISP)

methods within an acceptable range (Paatero et al., 2014); (vi) by obtaining modelled total variable (PNC) successfully predicted (R^2 > 0.9 and slopes ≈1); and (vii) by avoiding the presence of edges in the G-space plots (Paatero et al., 2002) and, then, the presence of hidden/unresolved sources.

The interpretation of PMF results was then attempted by considering: (i) the knowledge of sources impacting the study area; (ii) the comparison with the results reported by Vu et al. (2016), who performed a PMF analysis of SMPS data collected in North Kensington (London urban background); (iii) the shape of resulting profiles for both the particle number and volume concentrations; (iv) the analysis of diurnal patterns; (v) the directional analysis using the polar plot and CBPF; (vi) the correlations between the source contributions and the other air pollutants monitored at the site or with weather variables, and (vii) the analysis of possible remote source areas by applying the CWT model.

Six-factor solutions were extracted for both the seasons. The resulting factor profiles are presented in Figures 6 and 7 for the warm and cold season, respectively. The factor profiles are expressed as: (i) particle number concentrations and their DISP ranges; (ii) particle volume concentrations, and (iii) explained variations showing how much of the variance (from 0 to 1) in the original dataset is accounted for by each extracted factor. The figures also show the diurnal patterns and the polar plots computed on the hourly-averaged contributions. Table 1 summarises the PMF results and spectral characteristics, while Table 2 shows the Pearson correlation matrices with weather and air quality variables. Selected PMF solutions were very stable: no errors or unmapped factors and few swaps (none in summer and <7% in winter) were found in BS; no swaps or errors even at dQ_{max}=25 were found for DISP, i.e. solutions were affected by small rotational ambiguity and, therefore, their interpretation can be considered robust.

548 DISP analysis is designed to explore the realistic bounds on the optimal (base run) PMF solutions
549 that do not result in appreciable increases in the *Q* values (Brown et al., 2015). In this study, the
550 ranges calculated by DISP for the *dQ*=4 were used to assess the uncertainty boundaries associated
551 to the final PMF profiles, as suggested in Zikova et al. (2016) and Masiol et al. (2017). This
552 strategy is useful to better interpret the results, as the regions of spectra affected by high rotational
553 ambiguity are disclosed in the resulting profiles.
554
555 *3.3.1 Warm season*
556 *Factor 1* includes most of the particles in the nucleation range (<20 nm), exhibits a sharp mode in
557 the number distribution below the SMPS detection limit (14 nm) and makes the largest contribution
558 to the total PNC (31.6%, DISP range 31-36%) (Figure 6). However, its contribution to the volume
559 distribution is ~1%. Several studies report that particles in the nucleation range are emitted from the
560 aircraft engines (e.g., Anderson et al., 2005; Herndon et al., 2008; Kinsey et al., 2010; Mazaheri et
561 al., 2009;2013; Masiol and Harrison, 2014; Lobo et al., 2015) as well as from other anthropogenic
562 (e.g., Schneider et al., 2005; Chen et al., 2011; Cheung et al., 2012; Stevens et al., 2012; Kumar et
563 al., 2013;2014; Vu et al., 2015b) and natural (e.g., Kulmala et al., 1998; O'Dowd et al., 1998;1999;
564 Kulmala and Kerminen, 2008; Riccobono et al., 2014) sources. This factor does not show any
565 significant ($p < 0.05$) and strong ($r \geq |0.6|$) correlation with other measured species, but a weak ($|0.4|$
566 $\leq r < |0.6|$) correlation with Factor 2. Its diurnal variation (Figure 6) shows higher concentrations
567 between 6 am and 10 pm, and well agrees with the airport flight movements (Figure 2). The polar
568 plot analysis also indicates enhanced levels when winds > 2 m s^{-1} blow from the airfield sectors
569 (SW). All these insights are consistent with the location of Heathrow, i.e. the most plausible
570 interpretation is related to the aircraft engine exhaust emissions. This interpretation is also
571 supported by Keuken et al. (2015), which shows that the PNSD in an area affected by emissions
572 from Schiphol airport (The Netherlands) is dominated by ultrafine (10-20 nm) particles. The large
573 contribution of this factor to the total PNC is not surprising if compared to the results reported for

574 the Los Angeles international airport by Hudda et al. (2014) (emissions from the airport increased
575 PNC 4- to 5-fold at 8–10 km downwind the airfield). Since the airport of Los Angeles and LHR
576 have comparable aircraft traffic, the quite high concentrations found in this study (on annual
577 average nucleation particles are ~10 times higher than those measured in North Kensington urban
578 background by Vu et al. (2016)) are consistent with the sampling location chosen in this study (~1.2
579 km to the airfield). In addition, this result also agrees with previous studies on the impacts of LHR
580 on local air quality; Carslaw et al. (2006) and Masiol and Harrison (2015) found comparable
581 percent contributions of LHR emissions on NO_2 levels in the study area (approx. 25-30%).
582 However, the lack of correlations with NO and NO_2 (tracers for aircraft emissions) is probably due
583 to the difference in the time resolution and the presence of several other sources of nitrogen oxides
584 in the area, such as the heavy traffic generated from the airport and from the nearby motorways.
585
586 *Factor 2* is made up of ultrafine particles in the nucleation-Aitken range (one main peak at 20-35
587 nm) and accounts for 28% (DISP 25-30%) of PNC; its contribution to the volume distribution is
588 low (~2%) and peaks at 22-45 nm and at 140-220 nm. Several insights seem to link this factor to
589 road traffic emissions: (i) the modal structure; (ii) the strong association with morning and evening
590 rush hours, and (iii) the significant increase for winds in the west and south-westerly sectors
591 consistent with emissions generated from local busy roads close to LHR, Tunnel Rd. and M25
592 motorway. A similar mode in the nucleation range has been extensively attributed to the size
593 distribution from road traffic (e.g., Vogt et al., 2003; Zhang et al., 2004; Ntziachristos et al., 2007;
594 Vu et al., 2015b) and the growth of nucleation particles from diesel vehicles (Mayer and Ristovski,
595 2007; Wehner et al., 2009). For example, Charron and Harrison (2003) reported that particles in the
596 range 30–60 nm show a stronger association with light-duty traffic at a traffic hotspot in central
597 London (Marylebone Rd.); Janhäll et al. (2004) reported an average particle size distribution
598 peaking at 15-30 nm during morning peak high traffic intensity in the city of Göteborg (Sweden),
599 which has a car fleet comparable to the UK; Ntziachristos et al. (2007) found a sharp mode at 20-30

nm in sampling from engine exhausts. In addition, PMF factors with similar modal structures were found in other studies and were attributed to road traffic emissions: among others, Harrison et al. (2011) linked a factor peaking at 20 nm to primary road traffic emissions near a major UK highway; Masiol et al. (2016) measured PNSD in an international airport in Northern Italy during summer and interpreted a factor with a clear mode at 35-40 nm as road traffic from the nearby city; Beddows et al. (2015) and Vu et al. (2016) found traffic factors with modal diameter at around 30 nm in an urban background site in London (North Kensington); Sowlat et al. (2016) reported a factor peaking at 20–40 nm in number concentration and at around 30–40 nm in volume concentration in Los Angeles (US) and interpreted it as traffic tailpipe emissions. However, this factor lacks significant positive correlations with primary road traffic tracers (nitrogen oxides, eBC), while other studies have reported weak positive correlations with such species (Harrison et al., 2011; Masiol et al., 2016; Vu et al., 2016; Sowlat et al., 2016). Similarly to factor 1, this latter result may be due to the difference in the time resolution between chemical species and PNSD and the presence of several sources of nitrogen oxides in the area.

Factor 3 is mostly represented by 25–90 nm particles and contributes about 19% (17-21%) to the total number concentration. It also shows a second mode below the SMPS detection limit (14 nm), however, the DISP range clearly indicates that this part of the profile is affected by a large amount of rotational ambiguity, so that the presence of this second mode should be interpreted with caution. The volume concentration peaks at around 40–100 nm and 250–450 nm. The factor contribution is higher during rush hours, but the morning peak occurs 1 h later than in factor 2. The wind directionality shows increases for air masses blowing gently (<4 m s^{-1}) from W and for calm wind periods, suggesting a quite local source; however, also an increase of concentrations is found for higher wind regimes (>6 m s^{-1}) from the East (London). Factor 3 also shows significant positive correlations with NO (0.43) and NO_2 (0.61). All these insights seem to point to an aged road traffic source. This interpretation is also supported by Vu et al. (2016), who found a similar factor in

London (North Kensington) peaking at ~20–100 nm. In this context, several source apportionment studies on PNSDs have attributed more than one factor to road traffic (e.g. Kasumba et al., 2009; Thimmaiah et al., 2009; Harrison et al., 2011; Liu et al., 2014; Al-Dabbous and Kumar, 2015; Vu et al., 2016; Sowlat et al., 2016). This result is not surprising in areas where heavy traffic is widespread, as particles may undergo condensation, agglomeration, evaporation and dilution processes and, consequently, they may change modal characteristics in time and space. Such atmospheric processes are the main mechanisms reshaping PNSDs after primary exhausts are emitted into the atmosphere and have been discussed in several studies (Shi et al., 1999; Kim et al., 2004; Zhang et al., 2005; Zhou et al., 2005; Kulmala and Kerminen, 2008; Zhang et al., 2011; Harrison et al., 2016).

Factor 4 is made up of ultrafine particles over a wide range (50-200 nm with a clear mode at ~80 nm for PNC and 60-300 nm for PVC). The factor contributes 14% of PNC, but accounts for the main percentage of the volume concentration (33%). This factor well correlates with gaseous pollutants linked to combustion sources (mostly road traffic), i.e. NO (0.6), NO_2 (0.76), and non-volatile primary pollutants, such as eBC (0.61), $NVPM_{2.5}$ (0.62) and EC (0.75). The factor also strongly correlates with OC (0.84) and sulphate (0.75). The diurnal pattern shows two main peaks in the morning and evening rush hours, but the concentrations recorded between the two maxima are higher overnight than during daytime. This pattern suggests that both local emission sources and the dynamics of the mixing layer may play a key role in shaping its diurnal cycle, i.e. emitted pollutants undergo a wide dispersion within the expanded mixing layer during the daytime, while the drop of the mixing layer occurring overnight restricts those pollutants to a layer close to ground level. The polar plot indicates increased levels for wind calm or winds blowing from London (East sectors); in addition, the factor is strongly negatively correlated with wind speed (-0.64).

All these insights suggest that Factor 4 represents the fingerprint of the London pollution. Several studies carried out in London (Beddows et al., 2009;2015; Vu et al., 2016) and other megacities (e.g., New York: Masiol et al., 2017) have reported similar results, all interpreting this source profile as urban background (or urban accumulation mode). This source comprises both the solid particle mode from traffic emissions (Harrison et al., 2011; Pant and Harrison, 2013; Dall'Osto et al., 2012) and secondary species condensed upon pre-existing particles acting as condensation nuclei, including secondary sulphate, nitrate and organic aerosols. Secondary sulphate is formed through the atmospheric processing of local or distant SO_2 emissions (Kerminen et al., 2000) and neutralisation with ammonia (Benson et al., 2011). Nitrate aerosol is formed through the oxidation of NO_2 to nitrate and the consequent neutralization with ammonia (Seinfeld and Pandis, 2006) and occurs during both daytime and night-time; however the semivolatile nature of ammonium nitrate, makes its partitioning to the condensed-phase very weak. This behaviour also favours the occurrence of negative artefacts in filter-based sampling, which may explain the lack of significant correlations between the factor and the $PM_{2.5}$-bound nitrate (Table 2). On the contrary, the increase of the intensity of factor 4 during the night-time and the significant association with NO_2 are highly consistent with the chemistry driving the heterogeneous reactions of N_2O_5 and NO_3 on aerosol surfaces (Bertram and Thornton, 2009; Brown and Stutz, 2012). In view of this, Dall'Osto et al. (2009) reported that most nitrate particles in London are: (i) locally produced in urban locations during nighttime; (ii) mainly present in particles smaller than 300 nm and (iii) internally mixed with sulphate, ammonium, EC and OC.

Factors 5 and 6 make small contributions to PNC (4-7% and 1-4%, respectively), but are relevant for the volume concentration (37% and 21%, respectively). Factor 5 shows a main accumulation mode in number concentration at 110-250 nm and two more modes at ~30-70 nm and below 14 nm; however, the latter two modes suffer of large rotational ambiguity and should be interpreted with care. On the contrary, it exhibits a wide mode in volume concentration ranging from ~100 to ~500

677 nm. Factor 6 has two relevant modes in number concentration at 55-120 nm and 230-400 nm, and
678 two modes in volume concentration at 260-500 nm and 75-140 nm.
679
680 These factors still present two peaks corresponding to the rush hours, but the morning peak occurs
681 1-2 h earlier than in the road traffic-related factors, i.e. when ambient temperature reaches its daily
682 minimum. Both factors correlate well with secondary aerosol tracers (nitrate, sulphate, OC) and
683 non-volatile components (eBC, EC, $NVPM_{2.5}$), but Factor 6 exhibits much higher correlation
684 coefficients. Despite the polar plots indicating main wind directionality toward N-E sectors, the
685 analysis of air mass histories though the CWT model (Figure 8) clearly indicates likely continental
686 origin areas rather than local sources.
687
688 Vu et al. (2016) observed two factors in North Kensington with very similar modal structures, daily
689 patterns, correlations with $PM_{2.5}$-bound species and external source areas maps. Therefore, their
690 interpretation is confirmed also in this study, i.e. mixed secondary aerosol (Factor 5) and inorganic
691 secondary aerosol (Factor 6). Both factors are clearly originated from the continental Europe and
692 are consistent with a previous receptor modelling study carried out in a rural background site
693 representative of southern UK (Charron et al., 2013). Similar origin and formation mechanisms also
694 explain their strong correlation (0.75). Despite it is not reasonable extract more information from
695 these data due to the short period into account and the large uncertainty associated with back-
696 trajectory analysis, it can be observed that Factor 5 shows a wide source area all over the Central
697 Europe, while Factor 6 exhibits two distinct hotspots (Central and North-eastern Europe).
698
699 *3.3.2 Cold season*
700 The 6 factors identified during the cold period (Figure 7) are similar to those for the warm season.
701 *Factor 1* is composed of a high proportion of particles in the nucleation range with a sharp mode at
702 ~15 nm. It accounts for 33% (32-35%) of PNC and less than 2% of PVC. The polar plot reveals

703 increased concentrations for moderate winds blowing from the airport sector and the diurnal pattern
704 is also compatible with the aircraft traffic. No statistically significant correlations are found with
705 any other monitored species. Therefore, Factor 1 may be attributed to the airport emissions related
706 to the aircraft engine exhausts emissions. As in the warm season, factor 1 is moderately correlated
707 with factor 2 (fresh road traffic, r=0.55), indicating a quite clear relationship between the two
708 sources.
709
710 *Factor 2* represents particles in the 15-35 nm range of number concentration, accounting for 35%
711 (33-37%) of total PNC. Its importance for volume concentration is modest (3%) with two modes at
712 30 and 200 nm. The diurnal pattern and the wind directionality are compatible with LHR as a
713 source and it shows a weak positive correlation with NO_2 (0.42) and a strong correlation with
714 nitrate (0.63). Despite its similarity and relationship with Factor 1 and the consequent similar
715 potential origin, Factor 2 may represent a different source: Factors 1 and 2 remain clearly separated
716 even at solutions down to 4 factors, demonstrating their structural robustness and the lack of
717 potential artefacts upon the PMF solution. Consequently, it can be concluded that they to not
718 represent over-resolved solutions (i.e. factor splitting). The most plausible interpretation for Factor
719 2 is therefore the same as for the warm season, i.e. fresh road traffic emissions. Furthermore, this
720 factor can be attributed to the road traffic generated by the airport and nearby major roads.
721
722 *Factor 3* includes most of the particles in the Aitken range and accounts for 19% (18-20%) of PNC.
723 It contribution to particle volume concentration is relevant (9%) with a main peak at around 100 nm
724 and a secondary peak at 400 nm. It presents two rush hours peaks and the polar plot reveals an
725 origin from the SW quadrant. However, as with the warm period, the wind directionality suggests
726 increases for slower wind regimes than the fresh road traffic factor and for more westerly sectors,
727 which are not compatible with the airfield location. Since factor 3 well correlates with a number of
728 other pollutants linked to primary emissions from road traffic (NO (0.51), NO_2 (0.81), $PM_{2.5}$ (0.53),

729 OC (0.79) and EC (0.83)), it represents a second road traffic factor, more affected by aging in the
730 atmosphere than factor 2.
731
732 Despite the wind regimes from NE sectors being poorly represented during the cold campaign,
733 *Factor 4* is the only one showing a possible origin from London and for calm wind periods. As with
734 the warm season, it is composed of a wide range of particles encompassing the Aitken and
735 accumulation modes (50 to 150 nm), while the peak in volume concentration is at 170 nm. The
736 diurnal pattern is clearly related to the mixing layer dynamics and the correlation analysis reveals
737 strong relationships with many species (NO, NO_2, eBC, $NVPM_{2.5}$, OC, EC, nitrate, ammonium and
738 potassium). Consequently, it is concluded that it represents the urban accumulation mode, whose
739 contribution to the total volume concentration is also similar to the warm season (33%). It is
740 interesting to note the large similarity with the urban accumulation mode found in the warm season,
741 from which it differs slightly only in the diurnal pattern (higher overnight) and in the presence of a
742 strong correlation with nitrate (r=0.88), due to the lesser extent of negative artefacts on $PM_{2.5}$ filter
743 samples.
744
745 The last two factors are interpreted as due to secondary aerosols. Their modal structures, their
746 contributions to total PNC and PVC, and their correlations with $PM_{2.5}$-bound species largely reflect
747 the results obtained for the warm period. However, the CWT maps (Figure 8) highlight different
748 source areas, i.e. the origin of the secondary aerosols is regional (UK and Northern Europe). In
749 addition, the presence of strong positive correlations with chloride may also indicate a contribution
750 from the transport of sea-salt aerosol.
751
752 **3.3 Comparison of *k*-means and PMF**
753 The cluster analysis revealed the presence of 5 characteristic PNSD shapes during both the seasons.
754 These spectra have been linked to potential sources in the study area, i.e. road traffic, airport

activities, biomass burning and secondary aerosol formation processes. However, the cluster analysis is mostly driven by the size spectral regions with higher particle number concentrations, i.e. it has the disadvantage of partitioning the single observations predominantly according to the finest region of the size distribution. This limitation is well illustrated by the poor (almost null) separation of clusters based on the particle volume distributions (all clusters showed quite similar particle volume spectra). In addition, cluster analysis also has the disadvantage of linking each cluster to a single source and does not easily account for PNSD resulting from the mix of two or more different sources.

In contrast, the PMF analysis computed over the PNSD also accounts well for the sources with a small impact on the number distribution, but having a larger influence on the particle volume size distributions and, therefore, on the particle mass concentration. Despite the differences in the two methods, some further information can be extracted by combining the results of cluster and PMF analysis. Figure 9 shows the statistics of normalised PMF source contributions relating to each single cluster. Generally, the two methods well agree for the “airport” source, pointing out how much the airport-related emissions may shape the PNSD in the study area. For the warm period, significantly higher (0.05 significance) PMF contributions of the airport factor (F1) are measured for cluster 1, i.e. the airport fingerprint was well caught by both source apportionment methods. During the cold season, the airport factor (F1) is high during both clusters 1 and 5. While cluster 5 presents significant high PMF contributions only for factor 1, cluster 1 also shows high contributions of factor 2 (fresh road traffic). This result indicates that cluster 5 may be linked as the typical PNSD spectra for airport emissions, while cluster 2 likely represents mixed emissions from aircraft and airport-related traffic.

Results for fresh traffic emissions also agree between the two methods. Factors 2 exhibit the higher normalised contributions to clusters 5 and 1 for the warm and cold period, respectively. However, in

781 winter it is evident that PNSDs grouped on cluster 1 are also strongly influenced by airport
782 emissions, probably due to the lower mixing layer height and, thus, a lesser dispersion in the
783 atmosphere.
784
785 Clusters 4 for both the periods show enrichments in the contributions for 4 PMF sources (aged road
786 traffic, urban accumulation and the two secondary aerosols). This further emphasises that cluster 4
787 represents the typical PNSD during daytime resulting from the mixing of different sources. In a
788 similar way, clusters 3 and 2 in the warm and cold periods, respectively, represent the typical
789 nighttime spectra, i.e. they exhibit similar partitioning over the PMF sources and similar daily
790 cycles.
791
792 **3.4 Analysis of a Large Regional Nucleation Event**
793 Regional photochemical nucleation episodes are regularly recorded in the Southern and Eastern
794 UK. Their general characteristics have been reported in a number of studies (e.g., Alam et al., 2003;
795 Charron et al., 2007;2008; Beddows et al., 2015; Vu et al., 2016) and can be summarised as
796 follows: (i) particle modality at around 20 nm; (ii) higher frequency around noon in association with
797 the peak in actinic flux intensities; (iii) clear seasonal cycles (higher average contribution levels in
798 the summer, from June to September); (iv) marked directionality from the westerly sectors,
799 reflecting maritime atmospheric circulation regimes, with high wind speed and low $PM_{2.5}$
800 concentrations.
801
802 A strong regional nucleation event occurred during the warm period sampling campaign (starting on
803 7th September at 1 pm UTC and lasting for about 12 h). Increases of PNC were almost
804 simultaneously recorded at Harlington and at Harwell, a national network rural background site
805 located approx. 60 km WNW of LHR and representative of the regional background levels of air
806 pollution across the Southern UK. The comparison of PNC time series at the two sites is provided

807 as Figure SI7. Figure 10 shows the contour plots of SMPS data recorded at Harlington between 7th
808 and 8th September as well as the hourly averaged concentrations of nucleation, Aitken and
809 accumulation particles, TEOM-FDMS $PM_{2.5}$ mass and the contributions of Factors 1 to 4 extracted
810 by the PMF. The figure also reports the hourly counts of number of clusters extracted by the *k*-
811 means analysis. The contour plot shows a typical "banana" shape with particle mode growing from
812 ~20 nm (1 pm) to ~100 nm (overnight). The episode strongly influenced the PNSDs until around
813 midnight; however its effect is also visible over the first half of 8th September. The time series
814 (Figure 10) exhibits a clear peak in nucleation particles between 1 pm and 3 pm followed by peaks
815 of Aitken (3-11 pm) and accumulation mode (8 pm-2 am) particles. The back-trajectory analysis
816 (Figure 11) has revealed that the event occurred when north-westerly fresh (and clean) maritime air
817 masses were advected from the Atlantic. This is also supported by the $PM_{2.5}$ mass, which exhibited
818 a fast drop of concentrations just a few hours before the event, probably reducing the condensation
819 sink and facilitating nucleation.
820
821 Both atmospheric nucleation and aircraft engines are recognised to produce particles in the
822 nucleation range. The analysis of this single –but strong– episode gives insights into how much the
823 source apportionment results can potentially be affected by regional nucleation. This latter analysis
824 is possible because the wind directionality during the entire episode was from N sectors, i.e. the
825 contribution of LHR can be considered negligible.
826
827 The results of cluster analysis were just slightly affected by the event. Before the episode, the PNSD
828 spectra were mostly categorised as clusters 3 and 4 (urban background and daytime pollution,
829 respectively), while a few clusters (less than 1 h of observations) were categorised as "airport"
830 during the beginning of the episode. The growing of particles in the subsequent hours was then
831 identified as "fresh road traffic" (cluster 5) and "nighttime regional pollution" (cluster 2). In a

similar way, PMF results were slightly affected by the event, with a sharp increase of contribution levels for factor 1 (airport) and, then, for factors 2 (fresh road traffic) and 3 (aged road traffic).

This episode was the main nucleation event recorded during the two sampling campaigns. Other possible episodes also occurred (mostly during the warm season), but they were much less significant and often hard to detect. This qualitative analysis points to some conclusions: (i) regional photochemical nucleation events may have an effect on clustering and PMF results; (ii) the effect may lead to an "additive" bias, mostly over the "airport" and "road traffic" factors and clusters; (iii) the effect of regional nucleation events in the study area is largely overwhelmed by the strength of local sources, but in other locations with more frequent nucleation events it may be more important to identify and separate them.

4 CONCLUSIONS

The effect of airport emissions upon the particle number concentration and size distribution was assessed at a site close to a major European airport (Heathrow) serving a megacity (London). The conclusions to be drawn are:

- Anomalously high particle number concentrations were recorded for the finest sizes (nucleation <30 nm and Aitken nuclei 30-100 nm) if compared to an urban background site in London (N. Kensington).
- Polar plot analysis indicates that Heathrow is a strong potential source for NO_2, nucleation and Aitken particles, but its contribution to the mass concentration of $PM_{2.5}$ and eBC is very small. On the contrary, the London area seems to be a main source for PM and eBC.
- The *k*-means cluster analysis has revealed that 20% of PNSDs are mostly shaped by airport direct emissions, but particle size spectra are also strongly affected by other local sources (mostly fresh and aged road traffic during daytime) and the reduction of mixing layer depth

(during nighttime). Typical PNSD spectra have been identified for nighttime and daytime pollution as well. Such spectra are likely the result of multiple source mixtures.

- PMF analysis revealed that the fingerprint of Heathrow has a peculiar modal structure peaking at <20 nm. The direct airport emissions account for 30-35% of total particles in both the seasons. Such results are in line with percent estimations for NO_2 reported in previous studies.
- Other major contributors to PNC are fresh (24-36%) and aged (16-21%) road traffic emissions. Despite both applied source apportionment methods failing to fully disaggregate the emissions from the local traffic (including motorway) and traffic generated by the airport, results suggest that road traffic sources may contribute to the total PNC more than Heathrow (40-56%). However, making a clear distinction between the influence of traffic generated by the airport from other road traffic is not feasible from this analysis.
- The fingerprint of London has a wide mode between 50-150 nm. This urban accumulation mode accounts for around 10% of PNC and is the result of the advection of air masses from the city. It is more evident overnight due to the drop of the mixing layer top, the subsequent increase in air pollutants at ground level and the generation of nighttime secondary nitrate aerosols.
- Secondary sources accounted for less than 6% in number concentrations but for more than 50% in volume concentration. Long-range transport has a key role in advecting polluted air masses from mainland Europe.

ACKNOWLEDGEMNTS

The authors gratefully acknowledge: (i) the European Union for funding the Marie Curie Intra-European Fellowship for career development to M. Masiol through the project entitled ‘Chemical and Physical Properties and Source Apportionment of Airport Emissions in the context of European Air Quality Directives (Project CHEERS, call: FP7-PEOPLE-2012-IEF, project no. 328542); (ii) Heathrow Airport Ltd and Ricardo-AEA for supplying aircraft movement data and for the valuable

883 exchange of information and discussion, in particular Katherine Rolfe, Elizabeth Hegarty
884 (Heathrow), Brian Stacey (Ricardo-AEA) and David Vowles; (iii) DEFRA Automatic Urban and
885 Rural Network, and London Air Quality Network for providing pollutant data; (iv) Met Office and
886 BADC for weather data; (v) the NOAA Air Resources Laboratory (ARL) for the provision of the
887 HYSPLIT transport and dispersion model used in this publication; and (vi) Dr. Stefania Squizzato
888 (Clarkson University, USA) for the valuable exchange of information.

889

890

REFERENCES

ACI (Airport Council International): ACI releases preliminary world airport traffic rankings. Airports Council International, Montreal. Available at: http://www.aci.aero/News/Releases/Most-Recent/2016/04/04/ACI-releases-preliminary-world-airport-traffic-rankings- [last accessed: June 2016].

AEA: Heathrow Airport Air Quality Modelling for 2008/9: Results and Model Evaluation. Report by AEA Energy & Environment on behalf of BAA, July 2010. AEAT/ENV/R/2948/Issue 1.

Al-Dabbous, A. N., Kumar, P.: Source apportionment of airborne nanoparticles in a Middle Eastern city using positive matrix factorization, Environ. Sci. Process Impacts, 17, 802-812, 2015.

Alam, A., Shi, J. P. and Harrison, R. M.: Observations of new particle formation in urban air, J. Geophys. Res.,108, 4093-4107, 2003. doi:10.1029/2001JD001417

Anderson, B. E., Branham, H.-S., Hudgins, C. H., Plant, J. V., Ballenthin, J. O., Miller, T. M., Viggiano, A. A., Blake, D. R., Boudries, H., Canagaratna, M., Miake-Lye, R. C., Onasch, T., Wormhoudt, J., Worsnop, D., Brunke, K. E., Culler, S., Penko P., Sanders, T., Han, H.-S., Lee, P., Pui, D. Y. H., Thornhill, K. L., Winstead, E. L.: Experiment to Characterize Aircraft Volatile Aerosol and Trace-Species Emissions (EXCAVATE), NASA/TM-2005-213783, National Aeronautics and Space Administration, Hampton, VA., 2005.

Anttila, P., Tuovinen, J. P., Niemi, J. V.: Primary NO2 emissions and their role in the development of NO2 concentrations in a traffic environment, Atmos. Environ., 45, 986-992, 2011.

Atkinson, R. W., Fuller, G. W., Anderson, H. R., Harrison, R. M., Armstrong, B.: Urban ambient particle metrics and health: a time-series analysis, Epidemiol., 21, 501-511, 2010.

Beddows, D. C. S., Dall'Osto, M., Harrison, R. M.: Cluster analysis of rural, urban and curbside atmospheric particle size data, Environ. Sci. Technol., 43, 4694–4700, 2009.

Beddows, D. C. S., Dall'Osto, M., Harrison, R. M., Kulmala, M., Asmi, A., Wiedensohler, A., Laj, P., Fjaeraa, A. M., Sellegri, K., Birmili, W., Bukowiecki, N., Weingartner, E., Baltensperger, U., Zdimal, V., Zikova, N., Putaud, J.-P., Marinoni, A., Tunved, P., Hansson, H.-C., Fiebig, M., Kivekäs, N., Swietlicki, E., Lihavainen, H., Asmi, E., Ulevicius, V., Aalto, P. P., Mihalopoulos, N., Kalivitis, N., Kalapov, I., Kiss, G., de Leeuw, G., Henzing, B., O'Dowd, C., Jennings, S. G., Flentje, H., Meinhardt, F., Ries, L., Denier van der Gon, H. A. C., Visschedijk, A. J. H.: Variations in tropospheric submicron particle size distributions across the European continent 2008–2009, Atmos. Chem. Phys., 14, 4327-4348, 2014.

Beddows D. C. S., Harrison R. M., Green D. C. and Fuller G. W.: Receptor modelling of both particle composition and size distribution from a background site in London, UK., Atmos. Chem. Phys., 15, 10107-10125, 2015.

Belis, C. A., Larsen, B. R., Amato, F., El Haddad, I., Favez, O., Harrison, R. M., Hopke, P. K., Nava, S., Paatero, P., Prévôt, A., Quass, U., Vecchi, R. and Viana, M.: European guide on air pollution source apportionment with receptor models, JRC Reference Reports EUR26080 EN, 2014.

940 Benson, D. R., Yu, J. H., Markovich, A., Lee, S.-H.: Ternary homogeneous nucleation of H2SO4,
941 NH3, and H2O under conditions relevant to the lower troposphere, Atmos. Chem. Phys., 11, 4755-
942 4766, 2011.

943 Bertram, T. H. and Thornton, J. A.: Toward a general parameterization of N_2O_5 reactivity on
944 aqueous particles: the competing effects of particle liquid water, nitrate and chloride, Atmos. Chem.
945 Phys., 9, 8351-8363, 2009.
946
947 Bigi A and Harrison R. M.: Analysis of the air pollution climate at a central urban background site,
948 Atmos. Environ., 44, 2004-2012, 2010.
949
950 Brines, M., Dall'Osto, M., Beddows, D. C. S., Harrison, R. M. and Querol, X.: Simplifying aerosol
951 size distributions modes simultaneously detected at four monitoring sites during SAPUSS, Atmos.
952 Chem. Phys., 14, 2973-2986, 2014.
953
954 Brines, M., Dall'Osto, M., Beddows, D., Harrison, R., Gómez-Moreno, F., Núñez, L., Artíñano, B.,
955 Costabile, F., Gobbi, G. And Salimi, F.: Traffic and nucleation events as main sources of ultrafine
956 particles in high-insolation developed world cities, Atmos. Chem. Phys., 15, 5929-5945, 2015.
957
958 Brown, S. S. and Stutz, J.: Nighttime radical observations and chemistry, Chem. Soc. Rev., 41,
959 6405-6447, 2012.
960
961 Brown, S. G., Eberly, S., Paatero, P. and Norris, G. A.: Methods for estimating uncertainty in PMF
962 solutions: Examples with ambient air and water quality data and guidance on reporting PMF results,
963 Sci.Total Environ., 518, 626-635, 2015.
964
965 Carslaw, D. C. and Ropkins, K.: Openair - an R package for air quality data analysis, Environ.
966 Model. Softw., 27-28, 52-61, 2012.
967
968 Carslaw, D. C., Beevers, S. D., Ropkins, K. and Bell, M. C.: Detecting and quantifying aircraft and
969 other on-airport contributions to ambient nitrogen oxides in the vicinity of a large international
970 airport, Atmos. Environ., 40, 5424-5434, 2006.
971
972 Carslaw, D. C., Beevers, S. D. and Bell, M. C.: Risks of exceeding the hourly EU limit value for
973 nitrogen dioxide resulting from increased road transport emissions of primary nitrogen dioxide,
974 Atmos. Environ., 41, 2073-2082, 2007.
975
976 Chandrasekaran, S. R., Hopke, P. K., Newtown, M. and Hurlbut, A.: Residential-scale biomass
977 boiler emissions and efficiency characterization for several fuels, Energy & Fuels, 27, 4840-4849,
978 2013.
979
980 Charron, A. and Harrison, R. M.: Primary particle formation from vehicle emissions during exhaust
981 dilution in the roadside atmosphere, Atmos. Environ., 37, 4109–4119, 2003.
982
983 Charron, A., Degrendele, C., Laongsri, B. and Harrison, R. M.: Receptor modelling of secondary
984 and carbonaceous particulate matter at a southern UK site, Atmos. Chem. Phys. 13, 1879-1894,
985 2013.
986
987 Charron, A., Birmili, W. and Harrison, R. M.: Factors influencing new particle formation at the rural
988 site, Harwell, United Kingdom, J. Geophys. Res., 112, D14210, 2007. doi:10.1029/2007JD008425.
989
990

991 Charron, A., Birmili, W. and Harrison, R. M.: Fingerprinting particle origins according to their size
992 distribution at a UK rural site, J. Geophys. Res., 113, D07202, 2008. doi:10.1029/2007JD008562.
993
994 Chen, J. P., Tsai, T. S. and Liu, S. C.: Aerosol nucleation spikes in the planetary boundary layer,
995 Atmos. Chem. Phys., 11, 7171-7184, 2011.
996
997 Cheung, H. C., Morawska, L., Ristovski, Z. D., and Wainwright, D.: Influence of medium range
998 transport of particles from nucleation burst on particle number concentration within the urban
999 airshed, Atmos. Chem. Phys., 12, 4951-4962, 2012.
1000
1001 Clapp, L. J. and Jenkin, M. E.: Analysis of the relationship between ambient levels of O_3, NO_2 and
1002 NO as a function of NO_x in the UK, Atmos. Environ., 35, 6391-6405, 2001.
1003
1004 Costabile, F., Birmili, W., Klose, S., Tuch, T., Wehner, B., Wiedensohler, A., Franck, U.,
1005 Konig, K. and Sonntag, A.: Spatio-temporal variability and principal components of the particle
1006 number size distribution in an urban atmosphere, Atmos. Chem. Phys., 9, 3163-3195, 2009.
1007
1008 Cyrys, J., Eeftens, M., Heinrich, J., Ampe, C., Armengaud, A., Beelen, R., Bellander, T.,
1009 Beregszaszi, T., Birk, M., Cesaroni, G., Cirach, M., de Hoogh, K., De Nazelle, A., de Vocht, F.,
1010 Declercq C., Dedele, A., Dimakopoulou, K., Eriksen, K., Galassi, C., Grauleviciene, R., Grivas, G.,
1011 Gruzieva, O., Hagenbjörk Gustafsson, A., Hoffmann, B., Iakovides, M., Ineichen, A., Krämer, U.,
1012 Lanki, T., Lozano, P., Madsen, C., Meliefste, K., Modig, L., Mölterm, A., Mosler, G.,
1013 Nieuwenhuijsen, M., Nonnemacher, M., Oldenwening, M., Peters, A., Pontet, S., Probst-Hensch,
1014 N., Quass, U., Raaschou-Nielsen, O., Ranzi, A., Sugiri, D., Stephanou, E.G., Taimisto, P., Tsai, M.-
1015 Y., Vaskövi, E., Villani, S., Wang, M., Brunekreef, B. and Hoek, G.: Variation of NO2 and NO_x
1016 concentrations between and within 36 European study areas: Results from the ESCAPE study,
1017 Atmos. Environ., 62, 374-390, 2012.
1018
1019 Dall'Osto, M., Harrison, R. M., Coe, H., Williams, P. I. and Allan, J.D.: Real time chemical
1020 characterization of local and regional nitrate aerosols, Atmos. Chem. Phys., 9, 3709-3720, 2009.
1021
1022 Dall'Osto, M., Thorpe, A., Beddows, D. C. S., Harrison, R. M., Barlow, J. F., Dunbar, T., Williams,
1023 P.I. and Coe, H.: Remarkable dynamics of nanoparticles in the urban atmosphere, Atmos. Chem.
1024 Phys., 11, 6623-6637, 2011.
1025
1026 Dall'Osto, M., Beddows, D. C. S., Pey, J., Rodriguez, S., Alastuey, A., Harrison, R. M. and Querol,
1027 X.: Urban aerosol size distributions over the Mediterranean city of Barcelona, NE Spain, Atmos.
1028 Chem. Phys., 12, 10693-10707, 2012.
1029
1030 DEFRA: Air Pollution in the UK 2015. UK Department for Environment, Food and Rural Affairs.
1031 Issue of September 2016. Available at: https://uk-
1032 air.defra.gov.uk/assets/documents/annualreport/air_pollution_uk_2015_issue_1.pdf (last accessed:
1033 November 2016).
1034
1035 Dodson, R. E., Houseman, E. A., Morin, B. and Levy, J. I.: An analysis of continuous black carbon
1036 concentrations in proximity to an airport and major roadways, Atmos. Environ., 43, 3764-3773,
1037 2009.
1038
1039 Farias, F. and ApSimon, H.: Relative contributions from traffic and aircraft NO_x emissions to
1040 exposure in West London, Environ. Modell. Softw., 21, 477-485, 2006.
1041

Finlayson-Pitts, B. J. and Pitts Jr, J. N.: Chemistry of the upper and lower atmosphere: theory, experiments, and applications. Academic press, 2000.

Grice, S., Stedman, J., Kent, A., Hobson, M., Norris, J., Abbott, J., Cooke S.: Recent trends and projections of primary NO2 emissions in Europe, Atmos. Environ., 43, 2154-2167, 2009.

Harrison, R. M., Beddows, D. C. S. and Dall'Osto, M.: PMF Analysis of wide-range particle size spectra collected on a major highway, Environ. Sci. Technol., 45, 5522-5528, 2011.

Harrison, R. M., Beddows, D. C., Jones, A. M., Calvo, A., Alves, C. and Pio, C.: An evaluation of some issues regarding the use of aethalometers to measure woodsmoke concentrations, Atmos. Environ., 80, 540-548, 2013.

Harrison, R. M., Jones, A. M., Beddows, D. C. S., Dall'Osto, M. and Nikolova, I.: Evaporation of traffic-generated nanoparticles during advection from source, Atmos. Environ., 125, 1-7, 2016.

Herndon, S. C., Jayne, J. T., Lobo, P., Onasch, T. B., Fleming, G., Hagen, D. E., Whitefield, P. D. and Miake-Lye, R. C.: Commercial aircraft engine emissions characterization of in-use aircraft at Hartsfield-Jackson Atlanta International Airport, Environ. Sci. Technol., 42, 1877-1883, 2008.

Hopke, P. K.: Review of receptor modeling methods for source apportionment. JAWMA, 66, 237-259, 2016.

Hsu, H. H., Adamkiewicz, G., Houseman, E. A., Zarubiak, D., Spengler, J. D. and Levy, J. I.: Contributions of aircraft arrivals and departures to ultrafine particle counts near Los Angeles International Airport, Sci. Tot. Environ., 444, 347-355, 2013.

Hsu, H. H., Adamkiewicz, G., Houseman, E. A., Spengler, J. D., Levy and J.I.: Using mobile monitoring to characterize roadway and aircraft contributions to ultrafine particle concentrations near a mid-sized airport, Atmos. Environ., 89, 688-695, 2014.

Hudda, N., Gould, T., Hartin, K., Larson, T. V. and Fruin, S. A.: Emissions from an international airport increase particle number concentrations 4-fold at 10 km downwind, Environ. Sci. Technol., 48, 6628-6635, 2014.

Hudda, N., Simon, M. C., Zamore, W., Brugge, D. And Durant, J. L.: Aviation emissions impact ambient ultrafine particle concentrations in the greater Boston area, Environ.Sci. Technol., 50, 8514-8521, 2016.

Hussein, T., Molgaard, B., Hannuniemi, H., Martikainen, J., Jarvi, L., Wegner, T., Ripamonti, G., Weber, S., Vesala, T. and Hameri, K.: Fingerprints of the urban particle number size distribution in Helsinki, Finland: local vs. regional characteristics, Boreal Env. Res., 19, 1-20, 2014.

Janhäll S., Jonsson Å. M., Molnár P., Svensson E. A. and Hallquist M.: Size resolved traffic emission factors of submicrometer particles, Atmos. Environ., 38, 4331-4340, 2004.

Kasumba, J., Hopke, P. K., Chalupa, D. C. and Utell, M. J.: Comparison of sources of submicron particle number concentrations measured at two sites in Rochester, NY, Sci. Total Environ., 407, 5071-5084, 2009.

Kelly, F. J. and Fussell, J. C.: Size, source and chemical composition as determinants of toxicity attributable to ambient particulate matter, Atmos. Environ., 60, 504-526, 2012.

1094 Kerminen, V. M., Pirjola, L., Boy, M., Eskola, A., Teinilä, K., Laakso, L., Asmi, A., Hienola, J.,
1095 Lauri, A., Vainio, V. And Lehtinen, K.: Interaction between SO2 and submicron atmospheric
1096 particles, Atmos. Res., 54, 41-57, 2000.
1097
1098 Keuken, M. P., Moerman, M., Zandveld, P., Henzing, J. S. and Hoek, G.: Total and size-resolved
1099 particle number and black carbon concentrations in urban areas near Schiphol airport (the
1100 Netherlands), Atmos. Environ., 104 132-142, 2015.
1101
1102 Kim, E., Hopke, P. K., Larson, T. V. and Covert, D. S.: Analysis of ambient particle size
1103 distributions using unmix and positive matrix factorization, Environ. Sci. Technol., 38, 202-209,
1104 2004.
1105
1106 Kinsey, J. S., Dong, Y., Williams, D. C. and Logan, R.: Physical characterization of the fine
1107 particle emissions from commercial aircraft engines during the aircraft particle emissions
1108 experiment (APEX) 1 to 3, Atmos. Environ., 44, 2147-2156, 2010.
1109
1110 Kley, D., Kleinmann, M., Sanderman, H. and Krupa, S.: Photochemical oxidants: state of the
1111 science, Environ. Pollut., 100, 19-42, 1999.
1112
1113 Knibbs, L. D., Cole-Hunter, T. and Morawska, L.: A review of commuter exposure to ultrafine
1114 particles and its health effects, Atmos. Environ., 45, 2611-2622, 2011.
1115
1116 Kulmala, M., Toivonen, A., Mäkelä, J. M. and Laaksonen, A.: Analysis of the growth of nucleation
1117 mode particles observed in Boreal forest, Tellus B, 50, 449-462, 1998.
1118
1119 Kulmala, M. and Kerminen, V.-M.: On the formation and growth of atmospheric nanoparticles,
1120 Atmos. Res., 90, 132–150, 2008.
1121
1122 Kumar, P., Morawska, L., Birmili, W., Paasonen, P., Hu, M., Kulmala, M., Harrison, R. M.,
1123 Norford, L. and Britter, R.: Ultrafine particles in cities, Environ.Int., 66, 1-10, 2014.
1124
1125 Kumar, P., Pirjola, L., Ketzel, M. and Harrison, R M.: Nanoparticle emissions from 11 non-vehicle
1126 exhaust sources–A review, Atmos.Environ., 67, 252-277, 2013.
1127
1128 Lanzinger, S., Schneider, A., Breitner, S., Stafoggia, M., Erzen, I., Dostal, M., Pastorkova, A.,
1129 Bastian, S., Cyrys, J., Zscheppang, A. and Kolodnitska, T.: Associations between ultrafine and fine
1130 particles and mortality in five central European cities—Results from the UFIREG study, Environ.
1131 Int., 88, 44-52, 2016.
1132
1133 Lee, D. S., Fahey, D. W., Forster, P. M., Newton, P. J., Wit, R. C. N., Lim, L. L., Owen, B., Sausen
1134 and R.: Aviation and global climate change in the 21st century, Atmos. Environ., 43, 3520-3537,
1135 2009.
1136
1137 Liu, X., Wang, W., Liu, H., Geng, C., Zhang, W., Wang, H. and Liu, Z.: Number size distribution
1138 of particles emitted from two kinds of typical boilers in a coal-fired power plant in China, Eng.
1139 Fuels, 24, 1677-1681, 2010.
1140
1141 Liu, Z. R., Hu, B., Liu, Q., Sun, Y. and Wang, Y. S.: Source apportionment of urban fine particle
1142 number concentration during summertime in Beijing, Atmos. Environ., 96, 359-369, 2014.
1143

1144 Lobo, P., Hagen, D. E. and Whitefield, P. D.: Measurement and analysis of aircraft engine PM
1145 emissions downwind of an active runway at the Oakland International Airport, Atmos. Environ., 61,
1146 114-123, 2012.
1147
1148 Lobo, P., Hagen, D. E., Whitefield, P. D. and Raper, D.: PM emissions measurements of in-service
1149 commercial aircraft engines during the Delta-Atlanta Hartsfield Study, Atmos. Environ., 104, 237-
1150 245, 2015.
1151
1152 Lupu, A. and Maenhaut, W.: Application and comparison of two statistical trajectory techniques
1153 for identification of source regions of atmospheric aerosol species, Atmos. Environ., 36, 5607-5618,
1154 2002.
1155
1156 Masiol, M. and Harrison, R. M.: Aircraft engine exhaust emissions and other airport-related
1157 contributions to ambient air pollution: A review, Atmos. Environ., 95, 409-455, 2014.
1158
1159 Masiol, M. and Harrison, R.M.: Quantification of air quality impacts of London Heathrow Airport
1160 (UK) from 2005 to 2012, Atmos. Environ., 116, 308-319, 2015.
1161
1162 Masiol, M., Vu, V. T., Beddows, D. C. S. and Harrison, R.M.: Source apportionment of wide range
1163 particle size spectra and black carbon collected at the airport of Venice (Italy), Atmos. Environ.,
1164 139, 56-74, 2016.
1165
1166 Masiol M., Hopke P. K., Felton H. D., Frank B. P., Rattigan O. V., Wurth M. J. and LaDuke G. H.:
1167 Source apportionment of $PM_{2.5}$ chemically speciated mass and particle number concentrations in
1168 New York City, Atmos. Environ.,148, 215-229, 2017.
1169
1170 Mazaheri, M., Johnson, G. R. and Morawska, L.: Particle and gaseous emissions from commercial
1171 aircraft at each stage of the landing and takeoff cycle, Environ. Sci. Technol., 43, 441-446, 2009.
1172
1173 Mazaheri, M., Bostrom, T. E., Johnson, G. R. and Morawska, L.: Composition and morphology of
1174 particle emissions from in-use aircraft during takeoff and landing, Environ. Sci. Technol., 47, 5235-
1175 5242, 2013.
1176
1177 Meyer, N. K. and Ristovski, Z.: Ternary nucleation as a mechanism for the production of diesel
1178 nanoparticles: experimental analysis of the volatile and hygroscopic properties of diesel exhaust
1179 using the volatilization and humidification tandem differential mobility analyser, Environ. Sci.
1180 Technol., 41, 7309-7314, 2007.
1181
1182 Ntziachristos, L., Ning, Z. Geller, M. D. and Sioutas, C.: Particle concentration and characteristics
1183 near a major freeway with heavy-duty diesel traffic, Environ. Sci. Technol., 41, 2223-2230, 2007.
1184
1185 O'Dowd, C. D., Geever, M., Hill, M. K., Smith, M. H. and Jennings, S. G.: New particle formation:
1186 Nucleation rates and spatial scales in the clean marine coastal environment, Geophys. Res. Lett., 25,
1187 1661-1664, 1998.
1188
1189 O'Dowd, C., McFiggans, G., Creasey, D. J., Pirjola, L., Hoell, C., Smith, M. H., Allan, B. J., Plane,
1190 J. M. C., Heard, D. E., Lee, J. D., Pilling, M. J. and Kulmala, M.: On the photochemical production
1191 of new particles in the coastal boundary layer. Geophys. Res. Lett., 26, 1707-1710, 1999.
1192
1193 Ogulei, D., Hopke, P. K., Chalupa, D. C. and Utell, M. J.: Modeling source contributions to
1194 submicron particle number concentrations measured in Rochester, New York, Aerosol Sci.
1195 Technol., 41, 179-201, 2007.

1196 Ostro, B., Hu, J., Goldberg, D., Reynolds, P., Hertz, A., Bernstein, L. and Kleeman, M. J.:
1197 Associations of mortality with long-term exposures to fine and ultrafine particles, species and
1198 sources: Results from the California Teachers Study Cohort, Environ. Health Perspect., 123, 549-
1199 556, 2015.
1200
1201 Paatero, P.: Least squares formulation of robust non-negative factor analysis, Chemom. Intell. Lab.,
1202 37, 23-35, 1997.
1203
1204 Paatero,, P. and Tapper, U.: Positive matrix factorization: a non-negative factor model with optimal
1205 utilization of error estimates of data values, Environmetrics, 5, 111-126, 1994.
1206
1207 Paatero, P., Hopke, P. K., Song, X. H. and Ramadan, Z.: Understanding and controlling rotations in
1208 factor analytic models, Chemom. Intell. Lab. Syst.. 60, 253-264, 2002.
1209
1210 Paatero, P., Eberly, S., Brown, S. G. and Norris, G. A.: Methods for estimating uncertainty in
1211 factor analytic solutions., Atmos. Meas. Tech., 7, 781-797, 2014.
1212
1213 Pant, P. and Harrison, R. M.: Estimation of the contribution of road traffic emissions to particulate
1214 matter concentrations from field measurements: a review, Atmos. Environ., 77, 78-97, 2013.
1215
1216 Petzold, A., Ogren, J.A., Fiebig, M., Laj, P., Li, S.M., Baltensperger, U., Holzer-Popp, T., Kinne,
1217 S., Pappalardo, G., Sugimoto, N. and Wehrli, C.: Recommendations for reporting "black carbon"
1218 measurements. Atmos. Chem. Phys., 13, 8365-8379, 2013.
1219
1220 R Core Team: R: A language and environment for statistical computing. R Foundation for
1221 Statistical Computing, Vienna, Austria, 2015. URL http://www.R-project.org/.
1222
1223 Reff, A., Eberly, S. I. and Bhave, P. V.: Receptor modeling of ambient particulate matter data using
1224 positive matrix factorization: review of existing methods, JAWMA, 57, 146-154, 2007.
1225
1226 Riccobono, F., Schobesberger, S., Scott, C. E., Dommen, J., Ortega, I. K., Rondo, L., Almeida, J.,
1227 Amorim, A., Bianchi, F., Breitenlechner, M. And David, A.: Oxidation products of biogenic
1228 emissions contribute to nucleation of atmospheric particles, Science, 344, 717-721, 2014.
1229
1230 Rolph, G. D.: Real-time Environmental Applications and Display sYstem (READY) Website,
1231 http://www.ready.noaa.gov, NOAA Air Resources Laboratory, College Park, MD, 2016.
1232
1233 Salimi, F., Ristovski, Z., Mazaheri, M., Laiman, R., Crilley, L. R., He, C., Clifford, S. and
1234 Morawska, L.: Assessment and application of clustering techniques to atmospheric particle number
1235 size distribution for the purpose of source apportionment, Atmos. Chem. Phys., 14, 11883-11892,
1236 2014.
1237
1238 Salma, I., Füri, P., Németh, Z., Balásházy, I., Hofmann, W. and Farkas, Á.: Lung burden and
1239 deposition distribution of inhaled atmospheric urban ultrafine particles as the first step in their
1240 health risk assessment, Atmos. Environ., 104, 39-49, 2015.
1241
1242 Sandradewi, J., Prévôt, A. S., Szidat, S., Perron, N., Alfarra, M. R., Lanz, V. A., Weingartner, E.
1243 and Baltensperger, U.: Using aerosol light absorption measurements for the quantitative
1244 determination of wood burning and traffic emission contributions to particulate matter, Environ.
1245 Sci. Technol., 42, 3316-3323, 2008.
1246

Schneider, J., Hock, N., Weimer, S., Borrmann, S., Kirchner, U., Vogt, R. and Scheer, V.: Nucleation particles in diesel exhaust: Composition inferred from in situ mass spectrometric analysis, Environ. Sci. Technol., 39, 6153-6161, 2005.

Seinfeld, J. H. and Pandis, S. N.: Atmospheric Chemistry and Physics - From Air Pollution to Climate Change, second ed., John Wiley & Sons, New York, 2006.

Shi, J. P. and Harrison, R. M.: Investigation of ultrafine particle formation during diesel exhaust dilution, Environ. Sci. Technol., 33, 3730-3736, 1999.

Shi, L., Zanobetti, A., Kloog, I., Coull, B. A., Koutrakis, P., Melly, S. J. and Schwartz, J. D.: Low-concentration PM2. 5 and mortality: Estimating acute and chronic effects in a population-based study, Environ. Health Perspect., 124, 46-52, 2015.

Shirmohammadi, F., Sowlat, M. H., Hasheminassab, S., Saffari, A., Ban-Weiss, G. and Sioutas, C.: Emission rates of particle number, mass and black carbon by the Los Angeles International Airport (LAX) and its impact on air quality in Los Angeles, Atmos. Environ.,151, 82-93, 2017.

Sowlat M.H., Hasheminassab S. and Sioutas C.: Source apportionment of ambient particle number concentrations in central Los Angeles using positive matrix factorization (PMF), Atmos. Chem. Phys., 16, 4849-4866, 2016.

Squizzato, S. and Masiol, M.: Application of meteorology-based methods to determine local and external contributions to particulate matter pollution: A case study in Venice (Italy), Atmos. Environ., 119, 69-81, 2015.

Stein, A. F., Draxler, R. R, Rolph, G. D., Stunder, B. J. B., Cohen, M. D. and Ngan, F.: NOAA's HYSPLIT atmospheric transport and dispersion modeling system, Bull. Amer. Meteor. Soc., 96, 2059-2077, 2015.

Stevens, R. G., Pierce, J. R., Brock, C. A., Reed, M. K., Crawford, J. H., Holloway, J. S., Ryerson, T. B., Huey, L. G. and Nowak, J. B.: Nucleation and growth of sulfate aerosol in coal-fired power plant plumes: sensitivity to background aerosol and meteorology, Atmos. Chem. Phys., 12, 189-206, 2012.

Stohl A.: Trajectory statistics—a new method to establish source–receptor relationships of air pollutants and its application to the transport of particulate sulfate in Europe, Atmos. Environ., 30, 579-587, 1996.

Stohl, A.: Computation, accuracy and applications of trajectories- review and bibliography, Atmos. Environ., 32, 947-966, 1998.

Stafoggia, M., Cattani, G., Forastiere, F., di Bucchianico, A. D. M., Gaeta, A. And Ancona, C.: Particle number concentrations near the Rome-Ciampino city airport, Atmos. Environ., 147, 264-273, 2016.

Strak, M. M., Janssen, N. A., Godri, K. J., Gosens, I., Mudway, I. S., Cassee, F. R., Lebret, E., Kelly, F. J., Harrison, R. M., Brunekreef, B. and Steenhof, M.: Respiratory health effects of airborne particulate matter: the role of particle size, composition, and oxidative potential-the RAPTES project, Environ. Health Perspect., 120, 1183-1189, 2012.

1298 Thimmaiah, D., Hovorka, J. and Hopke, P. K.: Source apportionment of winter submicron Prague
1299 aerosols from combined particle number size distribution and gaseous composition data. Aerosol
1300 Air Qual.Res., 9, 209-236, 2009.
1301
1302 USEPA: EPA Positive Matrix Factorization (PMF) 5.0 - Fundamentals and user guide.
1303 EPA/600/R-14/108, 2014
1304
1305 Vogt, R., Scheer, V., Casati, R. and Benter, T.: Onroad measurement of particle emission in the
1306 exhaust plume of a diesel passenger car, Environ. Sci. Technol., 37, 4070-4076, 2003.
1307
1308 Vu, T. V., Delgado-Saborit, J. M. and Harrison, R. M.: A review of hygroscopic growth factors of
1309 submicron aerosols from different sources and its implication for calculation of lung deposition
1310 efficiency of ambient aerosols, Air Quality, Atmos. Health, 8, 429-440, 2015a.
1311
1312 Vu, T. V., Delgado-Saborit, J. M. and Harrison, R. M.: Review: Particle number size distributions
1313 from seven major sources and implications for source apportionment studies, Atmos. Environ., 122,
1314 114-132, 2015b.
1315
1316 Vu, T. V., Beddows, D. C. S., Delgado-Saborit, J. M. and Harrison, R. M.: Source Apportionment
1317 of the Lung Dose of Ambient Submicrometre Particulate Matter, Aerosol Air Quality Res., doi:
1318 10.4209/aaqr.2015.09.0553, 2016
1319
1320 Yin, J., Harrison, R. M., Chen, Q., Rutter, A. and Schauer, J. J.: Source apportionment of fine
1321 particles at urban background and rural sites in the UK atmosphere, Atmos. Environ., 44, 841-851,
1322 2010.
1323
1324 Yue, W., Stolzel, M., Cyrys, J., Pitz, M., Heinrich, J., Kreyling, W. G., Wichmann, H.-E.,Peters, A.,
1325 Wang, S. and Hopke, P.K.: Source apportionment of ambient fine particle size distribution using
1326 positive matrix factorization in Erfurt, Germany, Sci. Total Environ., 398, 133-144, 2008.
1327
1328 Wang, Y., Hopke, P. K., Rattigan, O. V., Xia, X., Chalupa, D. C., Utell, M. J.: Characterization of
1329 residential wood combustion particles using the two-wavelength aethalometer, Environ.Sci.
1330 Technol., 45, 7387-7393, 2011.
1331
1332 Webb, S., Whitefield, P. D., Miake-Lye, R. C., Timko, M. T. and Thrasher, T. G.: Research needs
1333 associated with particulate emissions at airports, ACRP Report 6, Transportation Research Board,
1334 Washington, D.C., 2008.
1335
1336 Wehner, B., Uhrner, U., Von Löwis, S., Zallinger, M. and Wiedensohler, A.: Aerosol number size
1337 distributions within the exhaust plume of a diesel and a gasoline passenger car under on-road
1338 conditions and determination of emission factors, Atmos. Environ., 43, 1235-1245, 2009.
1339
1340 Wegner, T., Hussein, T., Hämeri, K., Vesala, T., Kulmala, M. and Weber, S.: Properties of aerosol
1341 signature size distributions in the urban environment as derived by cluster analysis, Atmos.
1342 Environ., 61, 350-360, 2012.
1343
1344 Wormhoudt, J., Herndon, S. C., Yelvington, P. E., Lye-Miake, R. C. and Wey, C.: Nitrogen oxide
1345 (NO/NO2/HONO) emissions measurements in aircraft exhausts, J. Propul. Power, 23, 906-911,
1346 2007.
1347

1348 Zhang, K. M., Wexler, A. S., Zhu, Y. F., Hinds, W. C. and Sioutas, C.: Evolution of particle
1349 number distribution near roadways. Part II: the 'Road-to-Ambient'process, Atmos. Environ., 38,
1350 6655-6665, 2004.
1351
1352 Zhang, K. M., Wexler, A. S., Niemeier, D. A., Zhu, Y. F., Hinds, W. C. and Sioutas, C.: Evolution
1353 of particle number distribution near roadways. Part III: Traffic analysis and on-road size resolved
1354 particulate emission factors, Atmos. Environ., 39, 4155-4166, 2005.
1355
1356 Zhang, R., Khalizov, A., Wang, L., Hu, M. and Xu, W.: Nucleation and growth of nanoparticles in
1357 the atmosphere, Chem. Rev., 112, 1957-2011, 2011.
1358
1359 Zhou, L., Hopke, P. K., Stanier, C. O., Pandis, S. N., Ondov, J. M. and Pancras, J. P.: Investigation
1360 of the relationship between chemical composition and size distribution of airborne particles by
1361 partial least squares and positive matrix factorization, J. Geophys. Res.-Atmos., 110, D07S18, 2005,
1362 doi:10.1029/2004JD005050.
1363
1364 Zíková, N., Wang, Y., Yang, F., Li, X., Tian, M. and Hopke, P. K.: On the source contribution to
1365 Beijing PM 2.5 concentrations, Atmos. Environ., 134, 84-95, 2016.
1366
1367

TABLE LEGENDS:

Table 1. Summary of PMF results for both seasons.

Table 2. Results of Pearson's correlation analysis among extracted factor contributions and other measured variables recorded at different time resolutions. Only correlations significant at $p<0.05$ are reported, strong correlations ($\rho>|0.6|$) are highlighted in bold.

FIGURE LEGENDS:

Figure 1. Map of LHR and sampling site (left) and map of the Greater London area (upper right). Wind roses calculated over the two sampling periods are also provided (bottom right). The location of some main potential sources is also highlighted: T1, T2, T3, T4 and T5 are the Heathrow terminals; TR= Tunnel Rd.

Figure 2. Boxplots (a) and diurnal patterns (b) of the most important measured variables (and derived variables) during the two sampling periods. All valid data are used for computing boxplot statistics: Boxplot lines= medians, crosses= arithmetic means, boxes= 25th-75th percentile ranges, whiskers= ±1.5*inter-quartile ranges. Diurnal variations report the average levels as a filled line and the associated 95th confidence interval calculated by bootstrapping the data (n= 200). Outliers (data >99.5th percentile) were removed for computing the diurnal patterns. Hours are given in UTC. LHR traffic movements (bottom right plot) are reported as arrivals (dotted lines) and departures (solid lines). The offset between the seasons is largely due to daylight saving time (BST = UTC + 1) in the summer data.

Figure 3. Statistics of size distribution spectra for particle number (red) and volume (blue) concentrations categorised by sampling periods and time of the day (daytime= 7am-7pm and nighttime=7pm- 7am local time). For the particle number spectra, solid lines represent the median concentrations, while shaded areas report the 1st-3rd quartile intervals. For the particle volume spectra, only medians are reported (dotted lines).

Figure 4. Results of cluster analysis for the warm season data. Average cluster PNSD spectra (left) are reported as solid red lines along with: (i) their 10th, 25th, 75th and 90th percentile spectrum as shaded areas; (ii) the volume size distributions (dotted blue line); (iii) the hourly counts and (iv) the wind roses associated with each cluster.

Figure 5. Results of cluster analysis for the cold season data. Average cluster PNSD spectra (left) are reported as solid red lines along with: (i) their 10th, 25th, 75th and 90th percentile spectrum as shaded areas; (ii) the volume size distributions (dotted blue line); (iii) the hourly counts and (iv) the wind roses associated with each cluster.

Figure 6. Results of PMF analysis for the warm season data. Factor profiles are reported on the left as: (i) number concentration in solid red lines; (ii) their DISP ranges in shaded red areas; (iii) volume concentrations in dotted blue lines; (iv) explained variation in dashed grey lines. The plots on the centre report the normalised daily patterns calculated on the hourly-averaged factor contributions along with their 95th confidence intervals (n=200 bootstrap). The plots on the right show the polar plot analysis (normalised average factor contributions). SA=secondary aerosol.

Figure 7. Results of PMF analysis for the cold season data. Factor profiles are reported on the left as: (i) number concentration in solid red lines; (ii) their DISP ranges in shaded red areas; (iii) volume concentrations in dotted blue lines; (iv) explained variation in dashed grey lines. The plots on the centre report the normalised daily patterns calculated on the hourly-averaged factor contributions along with their 95th confidence intervals (n=200 bootstrap). The plots on the right show the polar plot analysis (normalised average factor contributions). SA=secondary aerosol.

Figure 8. CWT maps of the secondary aerosol-related factors for both the seasons. Map scales refer to the average factor contributions to the total variable (PNC).

Figure 9. Comparison of k-means and PMF for the warm (upper plots) and cold (bottom plots) seasons. Boxplot statistics: lines= medians, crosses= arithmetic means, boxes= 25th-75th percentile ranges, whiskers= ±1.5*inter-quartile ranges.

Figure 10. Analysis of the regional nucleation episode occurring on September 7th. The selected period is from 7 September midnight to 8 September 4 pm. The plots represent (from upper to the bottom): (a) contour plots of SMPS data; (b) Concentrations of some measured species (Nucl= particles in the nucleation range 14-30 nm; Ait= particles in the Aitken Nuclei range 30-100 nm; Acc= particles in the accumulation range >100 nm; mass of $PM_{2.5}$); (c) Source contributions from PMF for the Factors 1, 2, 3 and 4; (d) hourly counts of number of clusters. The arrows in the (b) and (c) plots show the wind direction (arrow direction) and speed (proportional to arrow length).

Figure 11. Backward air mass trajectories during the nucleation event. Dots indicate 24 h step times

Atmos. Chem. Phys. Discuss., doi:10.5194/acp-2017-150, 2017
Manuscript under review for journal Atmos. Chem. Phys.
Discussion started: 26 April 2017

Atmospheric Chemistry and Physics Discussions

1447 **Table 1**. Summary of PMF results for both seasons.

1448

Factor number and interpretation	Particle Number Concentration		Particle Volume Concentration	
Warm season (Aug-Sep 2014)	No. modes[a] (peak ranges[b])	Percent contribution (DISP range)	No. modes[a] (peak ranges[b])	Percent contribution
Factor 1: Airport	1 (<20 nm)	31.6 (30.8–36.2)	2 (60–160 nm; <25 nm)	1.2
Factor 2: Fresh road traffic	1 (20–35 nm)	27.9 (24.7–30.2)	2 (22–45 nm; 140–220 nm)	1.7
Factor 3: Aged road traffic	1 (30–60 nm)	18.9 (16.6–21.1)	2 (40–100 nm; 250–450 nm)	5.6
Factor 4: Urban accumulation	1 (50–150 nm)	14.4 (13.8–18)	1 (80–250 nm)	33.2
Factor 5: Mixed SA	1 (110–250 nm)	5.2 (3.6–6.9)	1 (160–350 nm)	37.4
Factor 6: Inorganic SA	2 (55–120 nm; 230–400 nm)	2.1 (1.1–3.5)	2 (260–500 nm; 75–140 nm)	20.8
Cold season (Dec 2014-Jan 2015)				
Factor 1: Airport	1 (<20 nm)	33.1 (31.7–34.8)	2 (160–350 nm; 15–25 nm)	1.7
Factor 2: Fresh road traffic	1 (18–35 nm)	35.2 (33.4–36.9)	2 (22–45 nm; 150–300 nm)	3.1
Factor 3: Aged road traffic	1 (28–60 nm)	18.9 (17.9–19.7)	2 (40–150 nm; 330–450 nm)	8.7
Factor 4: Urban accumulation	1 (55–170 nm)	7.6 (7.3–8.3)	1 (100–250 nm)	32.5
Factor 5: Mixed SA	2 (130–280 nm, <17 nm)	2.3 (2.1–3.3)	1 (170–400 nm)	30.8
Factor 6: Inorganic SA	3 (17–28 nm; 55–100 nm, 250–400 nm)	2.9 (2.4–3.9)	2 (280–550 nm; 90–140 nm)	23.3

(a) Only modes above the DISP ranges are shown; (b) Range endpoints are taken at approx. half the mode height.

1449

Atmos. Chem. Phys. Discuss., doi:10.5194/acp-2017-150, 2017
Manuscript under review for journal Atmos. Chem. Phys.
Discussion started: 26 April 2017

Atmospheric Chemistry and Physics Discussions

1450 **Table 2**. Results of Pearson's correlation analysis among extracted factor contributions and other
1451 measured variables recorded at different time resolutions. Only correlations significant at $p<0.05$
1452 are reported, strong correlations ($\rho>|0.6|$) are highlighted in bold.

1453

	Warm period					
	Factor 1	**Factor 2**	**Factor 3**	**Factor 4**	**Factor 5**	**Factor 6**
Variables	Airport	Fresh road traffic	Aged road traffic	Urban accumulation	Mixed SA	Inorganic SA
Weather parameters (1 h-resolution time)						
Solar irr.	0.12	-0.15	-0.24	-0.26	-0.24	-0.28
Air temp.	0.25	-0.21	-0.37	-0.1	0.1	
RH		0.1	0.32	0.22	0.26	0.33
Wind speed	0.38		-0.47	**-0.64**	-0.45	-0.49
5 min-resolution time						
Factor 1	–					
Factor 2	0.46	–				
Factor 3	0.03	0.28	–			
Factor 4	-0.17	-0.04	0.47	–		
Factor 5	-0.15	-0.06	0.21	0.56	–	
Factor 6	-0.17	-0.14	0.15	0.56	**0.75**	–
eBC	-0.1	-0.03	0.32	**0.61**	0.54	0.55
Delta-C			-0.06	-0.09	-0.12	-0.13
1 h-resolution time						
NO			0.43	**0.6**	0.32	0.33
NO_2		0.18	**0.61**	**0.76**	0.52	0.52
NO_x		0.11	0.58	**0.77**	0.48	0.48
O_3	0.14	-0.19	-0.57	-0.54	-0.37	-0.43
$PM_{2.5}$	-0.23	-0.24	0.13	**0.61**	**0.63**	**0.77**
$NVPM_{2.5}$	-0.22	-0.22	0.17	**0.62**	**0.61**	**0.75**
$VPM_{2.5}$	-0.17	-0.24		0.42	0.54	**0.65**
1 day-resolution time $PM_{2.5}$-bound species						
OC				**0.84**	**0.74**	**0.83**
EC	-0.47	-0.54		**0.75**	0.51	**0.67**
TC	-0.45	-0.44		**0.85**	**0.69**	**0.82**
Chloride						
Nitrate		-0.45			**0.83**	**0.85**
Sulphate		-0.57		**0.75**	0.5	**0.67**
Oxalate		-0.47		0.59	**0.89**	**0.93**
Sodium						
Ammonium	-0.44	-0.52		0.57	0.54	**0.71**
Potassium		-0.47		0.46	0.5	**0.66**
Magnesium	0.5			-0.53		
Calcium						

1454

Atmos. Chem. Phys. Discuss., doi:10.5194/acp-2017-150, 2017
Manuscript under review for journal Atmos. Chem. Phys.
Discussion started: 26 April 2017

Atmospheric Chemistry and Physics Discussions

1455 **Table 2**. Continued.

1456

	Cold period					
	Factor 1	**Factor 2**	**Factor 3**	**Factor 4**	**Factor 5**	**Factor 6**
Variables	Airport	Fresh road traffic	Aged road traffic	Urban accumulation	Mixed SA	Inorganic SA
Weather parameters (1 h-resolution time)						
Solar irr.				-0.11		
Air temp.	0.38		-0.43	**-0.67**	-0.5	-0.59
RH			0.23	0.38	0.46	0.46
Wind speed	0.3		-0.49	**-0.67**	-0.54	**-0.61**
5 min-resolution time						
Factor 1	–					
Factor 2	0.55	–				
Factor 3	0.24	0.54	–			
Factor 4	-0.11	0.08	0.53	–		
Factor 5	-0.05	0.15	0.38	**0.65**	–	
Factor 6	-0.09	0.08	0.39	**0.7**	**0.81**	–
eBC		0.19	0.54	**0.75**	0.57	**0.61**
Delta-C			0.1	0.21	0.22	0.19
1 h-resolution time						
NO	-0.14		0.51	**0.81**	**0.62**	**0.63**
NO_2	0.13	0.42	**0.81**	**0.82**	**0.61**	**0.66**
NO_x		0.17	**0.63**	**0.85**	**0.64**	**0.68**
O_3		-0.29	**-0.71**	**-0.78**	**-0.65**	**-0.7**
$PM_{2.5}$	-0.1	0.16	0.53	**0.82**	**0.88**	**0.88**
$NVPM_{2.5}$	-0.11	0.16	0.53	**0.82**	**0.85**	**0.85**
$VPM_{2.5}$			0.19	0.39	0.49	0.48
1 day-resolution time $PM_{2.5}$-bound species						
OC			**0.79**	**0.79**	**0.76**	**0.8**
EC			**0.83**	**0.8**	**0.64**	**0.66**
TC			**0.81**	**0.8**	**0.73**	**0.77**
Chloride				0.58	**0.82**	**0.85**
Nitrate		**0.63**	**0.73**	**0.88**	**0.93**	**0.9**
Sulphate					**0.92**	**0.88**
Oxalate					**0.87**	**0.81**
Sodium		-0.58	**-0.74**	**-0.64**		
Ammonium			**0.63**	**0.78**	**0.99**	**0.97**
Potassium				**0.71**	**0.98**	**0.97**
Magnesium						
Calcium						

1457
1458
1459

Atmos. Chem. Phys. Discuss., doi:10.5194/acp-2017-150, 2017
Manuscript under review for journal Atmos. Chem. Phys.
Discussion started: 26 April 2017

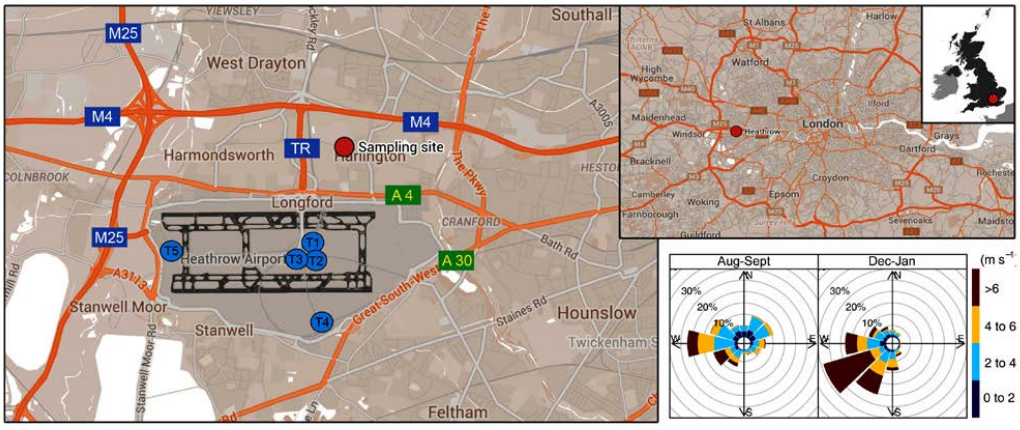

Figure 1. Map of LHR and sampling site (left) and map of the Greater London area (upper right). Wind roses calculated over the two sampling periods are also provided (bottom right). The location of some main potential sources is also highlighted: T1, T2, T3, T4 and T5 are the Heathrow terminals; TR= Tunnel Rd.

Atmos. Chem. Phys. Discuss., doi:10.5194/acp-2017-150, 2017
Manuscript under review for journal Atmos. Chem. Phys.
Discussion started: 26 April 2017

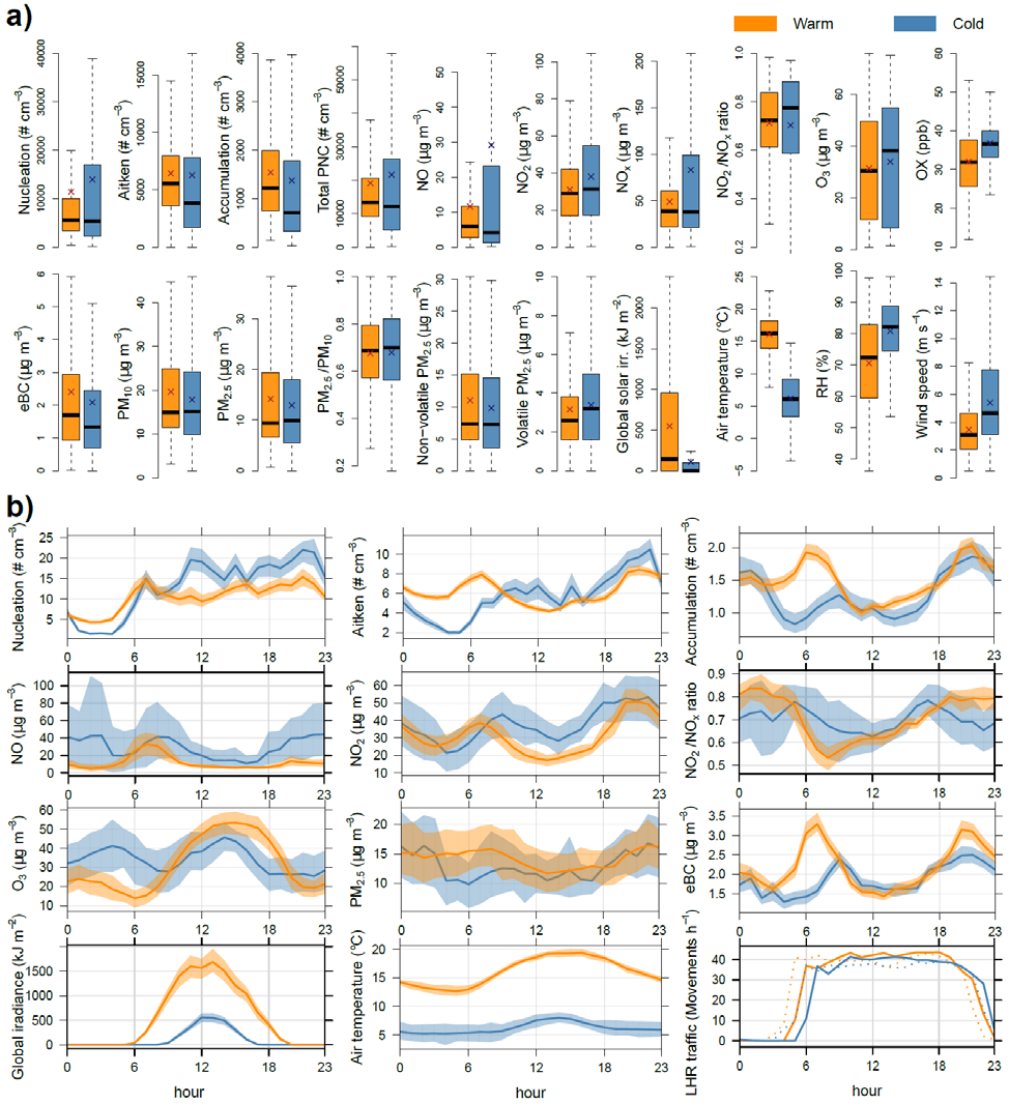

Figure 2. Boxplots (a) and diurnal patterns (b) of the most important measured variables (and derived variables) during the two sampling periods. All valid data are used for computing boxplot statistics: Boxplot lines= medians, crosses= arithmetic means, boxes= 25th-75th percentile ranges, whiskers= ±1.5*inter-quartile ranges. Diurnal variations report the average levels as a filled line and the associated 95th confidence interval calculated by bootstrapping the data (n= 200). Outliers (data >99.5th percentile) were removed for computing the diurnal patterns. Hours are given in UTC. LHR traffic movements (bottom right plot) are reported as arrivals (dotted lines) and departures (solid lines). The offset between the seasons is largely due to daylight saving time (BST = UTC + 1) in the summer data.

Atmos. Chem. Phys. Discuss., doi:10.5194/acp-2017-150, 2017
Manuscript under review for journal Atmos. Chem. Phys.
Discussion started: 26 April 2017

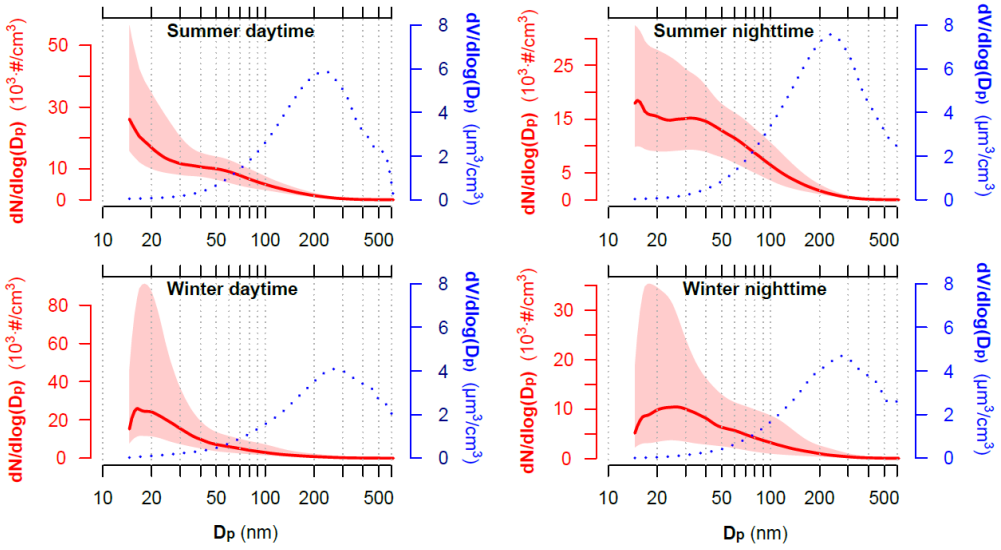

Figure 3. Statistics of size distribution spectra for particle number (red) and volume (blue) concentrations categorised by sampling periods and time of the day (daytime= 7am-7pm and nighttime=7pm- 7am local time). For the particle number spectra, solid lines represent the median concentrations, while shaded areas report the 1st-3rd quartile intervals. For the particle volume spectra, only medians are reported (dotted lines).

Atmos. Chem. Phys. Discuss., doi:10.5194/acp-2017-150, 2017
Manuscript under review for journal Atmos. Chem. Phys.
Discussion started: 26 April 2017

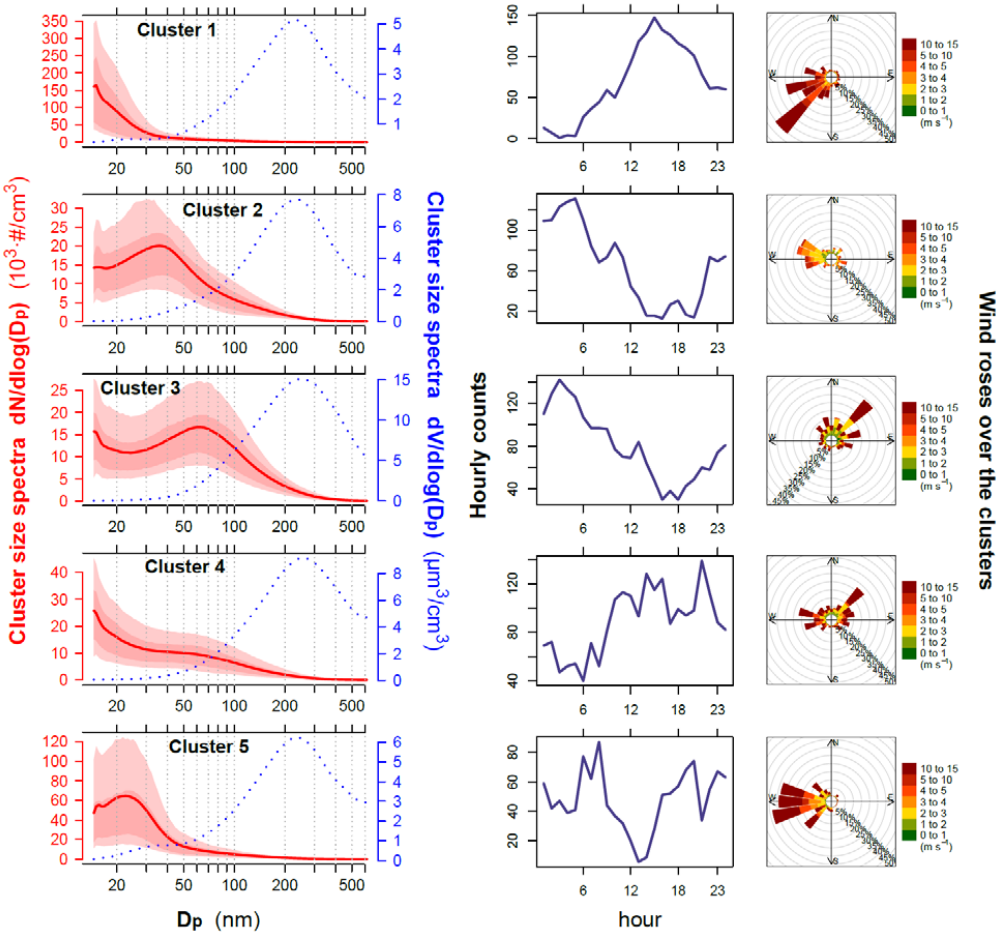

Figure 4. Results of cluster analysis for the warm season data. Average cluster PNSD spectra (left) are reported as solid red lines along with: (i) their 10th, 25th, 75th and 90th percentile spectrum as shaded areas; (ii) the volume size distributions (dotted blue line); (iii) the hourly counts and (iv) the wind roses associated with each cluster.

Atmos. Chem. Phys. Discuss., doi:10.5194/acp-2017-150, 2017
Manuscript under review for journal Atmos. Chem. Phys.
Discussion started: 26 April 2017

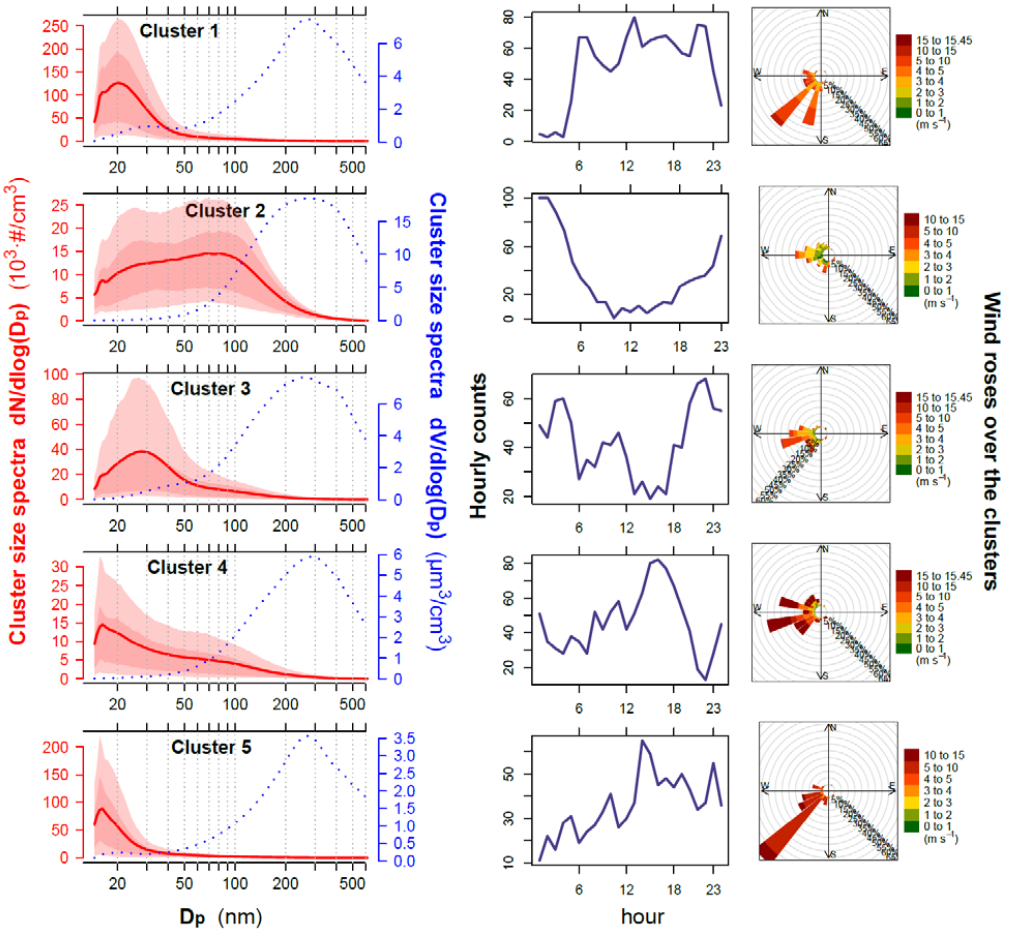

Figure 5. Results of cluster analysis for the cold season data. Average cluster PNSD spectra (left) are reported as solid red lines along with: (i) their 10th, 25th, 75th and 90th percentile spectrum as shaded areas; (ii) the volume size distributions (dotted blue line); (iii) the hourly counts and (iv) the wind roses associated with each cluster.

Atmos. Chem. Phys. Discuss., doi:10.5194/acp-2017-150, 2017
Manuscript under review for journal Atmos. Chem. Phys.
Discussion started: 26 April 2017

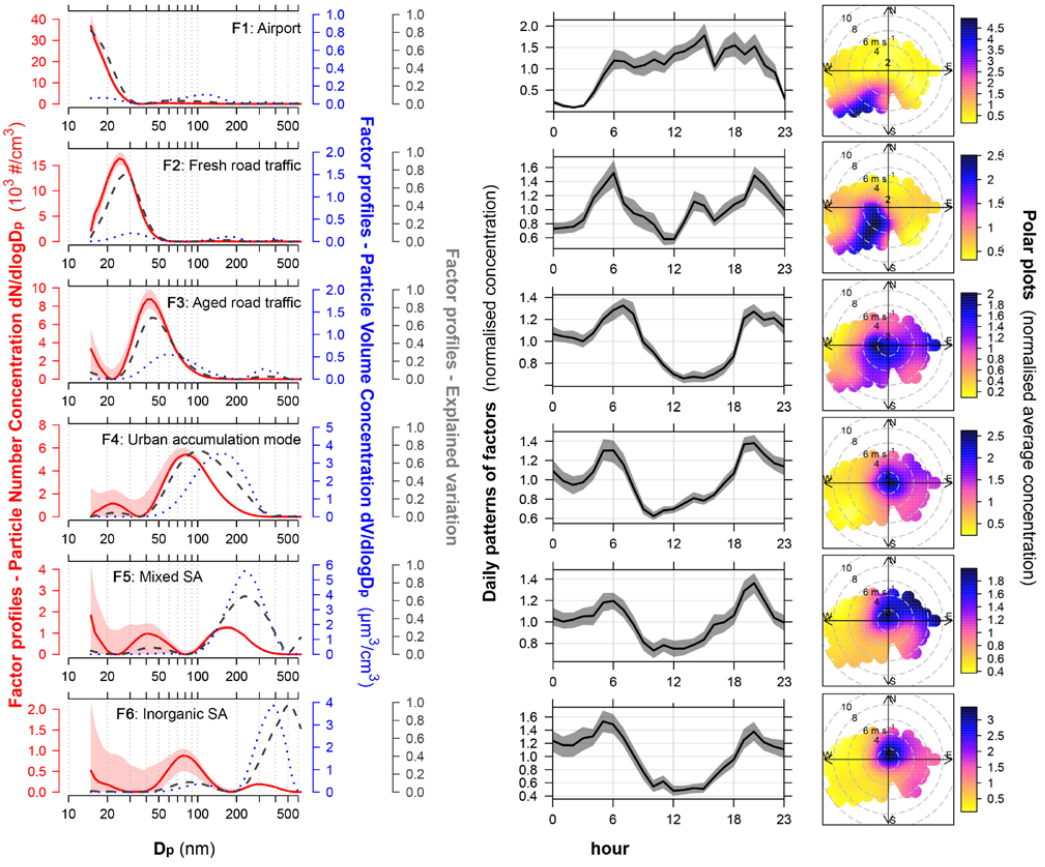

Figure 6. Results of PMF analysis for the warm season data. Factor profiles are reported on the left as: (i) number concentration in solid red lines; (ii) their DISP ranges in shaded red areas; (iii) volume concentrations in dotted blue lines; (iv) explained variation in dashed grey lines. The plots on the centre report the normalised daily patterns calculated on the hourly-averaged factor contributions along with their 95th confidence intervals (n=200 bootstrap). The plots on the right show the polar plot analysis (normalised average factor contributions). SA=secondary aerosol.

Atmos. Chem. Phys. Discuss., doi:10.5194/acp-2017-150, 2017
Manuscript under review for journal Atmos. Chem. Phys.
Discussion started: 26 April 2017

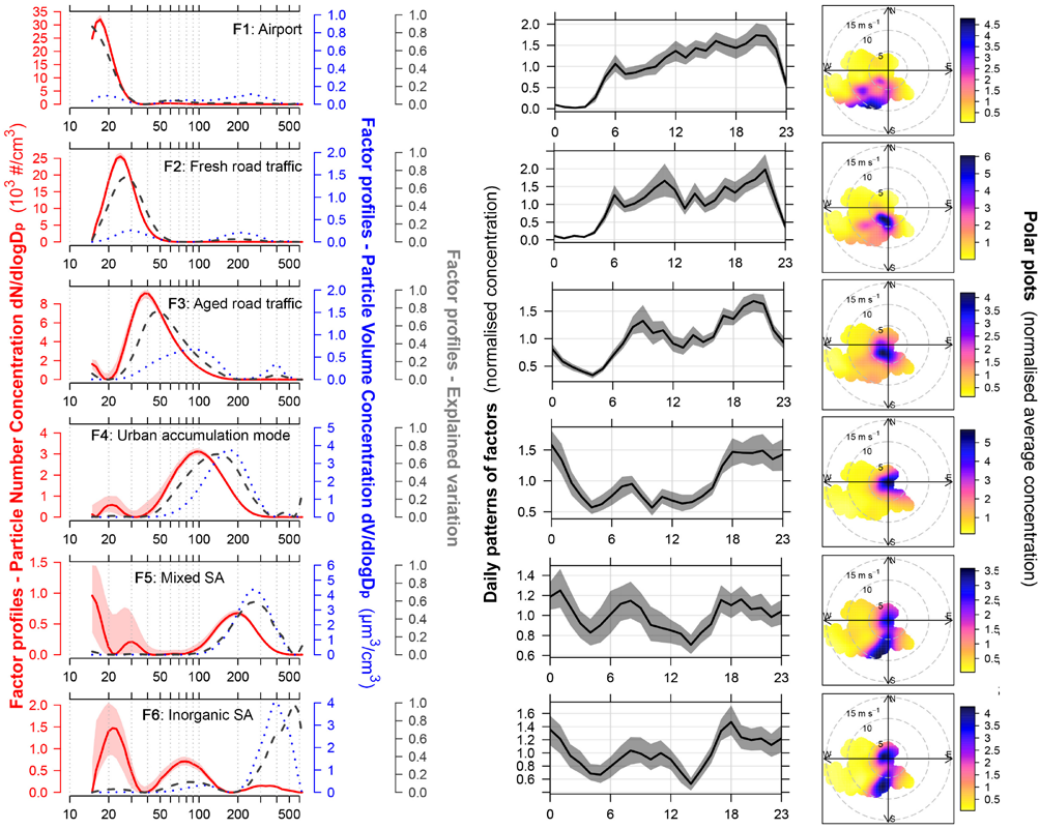

Figure 7. Results of PMF analysis for the cold season data. Factor profiles are reported on the left as: (i) number concentration in solid red lines; (ii) their DISP ranges in shaded red areas; (iii) volume concentrations in dotted blue lines; (iv) explained variation in dashed grey lines. The plots on the centre report the normalised daily patterns calculated on the hourly-averaged factor contributions along with their 95th confidence intervals (n=200 bootstrap). The plots on the right show the polar plot analysis (normalised average factor contributions). SA=secondary aerosol.

Atmos. Chem. Phys. Discuss., doi:10.5194/acp-2017-150, 2017
Manuscript under review for journal Atmos. Chem. Phys.
Discussion started: 26 April 2017

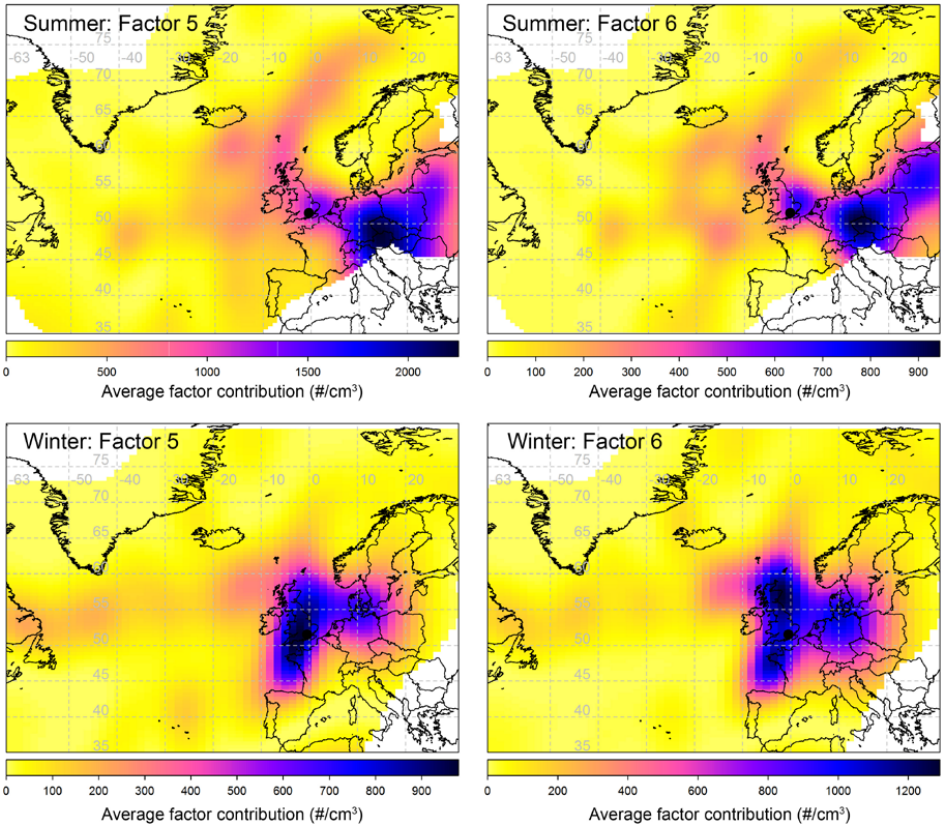

Figure 8. CWT maps of the secondary aerosol-related factors for both the seasons. Map scales refer to the average factor contributions to the total variable (PNC).

Atmos. Chem. Phys. Discuss., doi:10.5194/acp-2017-150, 2017
Manuscript under review for journal Atmos. Chem. Phys.
Discussion started: 26 April 2017

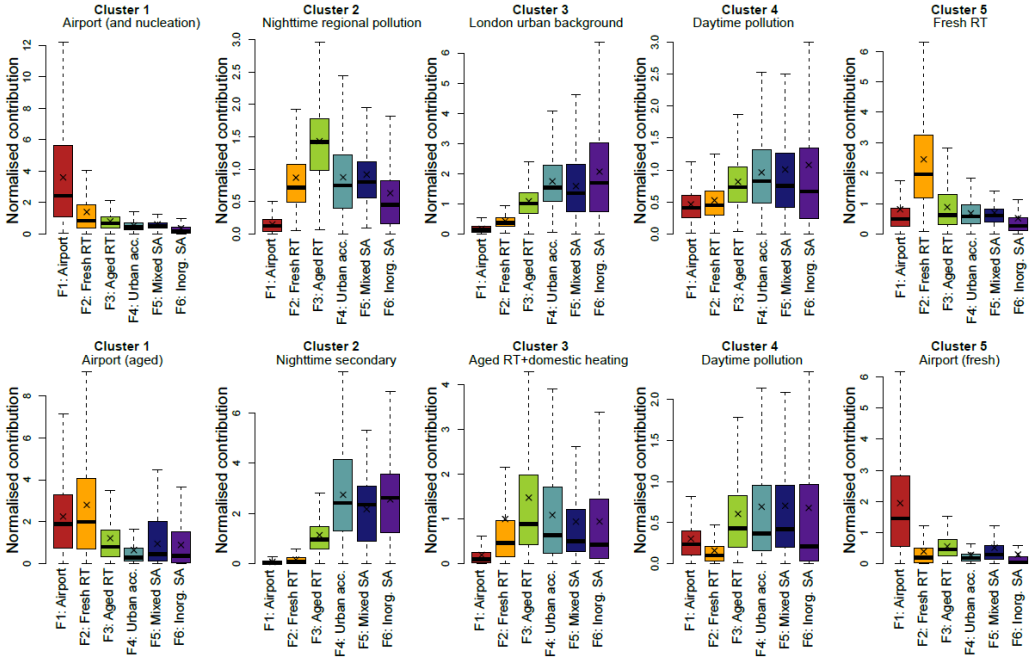

Figure 9. Comparison of k-means and PMF for the warm (upper plots) and cold (bottom plots) seasons. Boxplot statistics: lines= medians, crosses= arithmetic means, boxes= 25th-75th percentile ranges, whiskers= ±1.5*inter-quartile ranges.

Atmos. Chem. Phys. Discuss., doi:10.5194/acp-2017-150, 2017
Manuscript under review for journal Atmos. Chem. Phys.
Discussion started: 26 April 2017

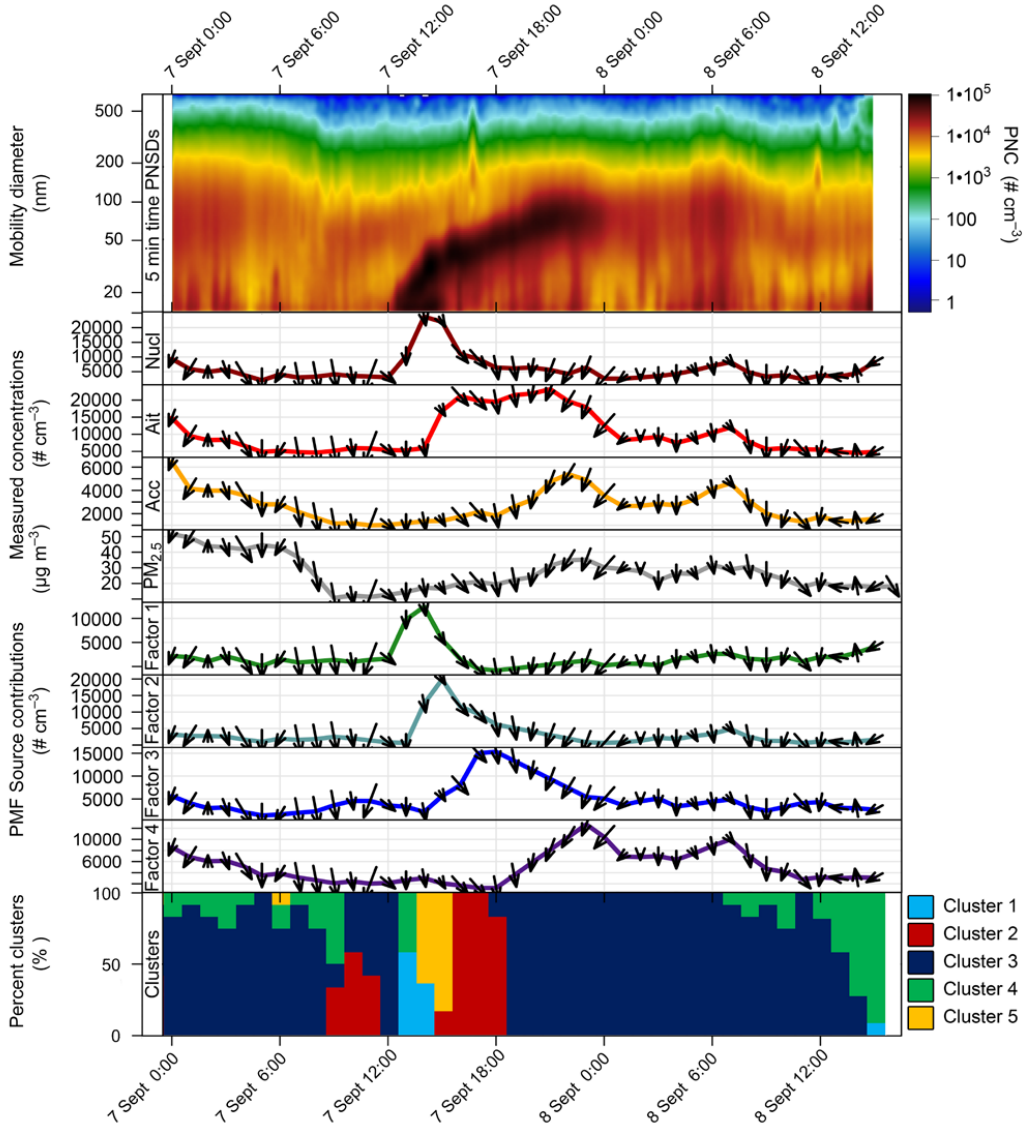

Figure 10. Analysis of the regional nucleation episode occurring on September 7th. The selected period is from 7 September midnight to 8 September 4 pm. The plots represent (from upper to the bottom): (a) contour plots of SMPS data; (b) Concentrations of some measured species (Nucl= particles in the nucleation range 14-30 nm; Ait= particles in the Aitken Nuclei range 30-100 nm; Acc= particles in the accumulation range >100 nm; mass of $PM_{2.5}$); (c) Source contributions from PMF for the Factors 1, 2, 3 and 4; (d) hourly counts of number of clusters. The arrows in the (b) and (c) plots show the wind direction (arrow direction) and speed (proportional to arrow length).

Atmos. Chem. Phys. Discuss., doi:10.5194/acp-2017-150, 2017
Manuscript under review for journal Atmos. Chem. Phys.
Discussion started: 26 April 2017

Atmospheric Chemistry and Physics Discussions

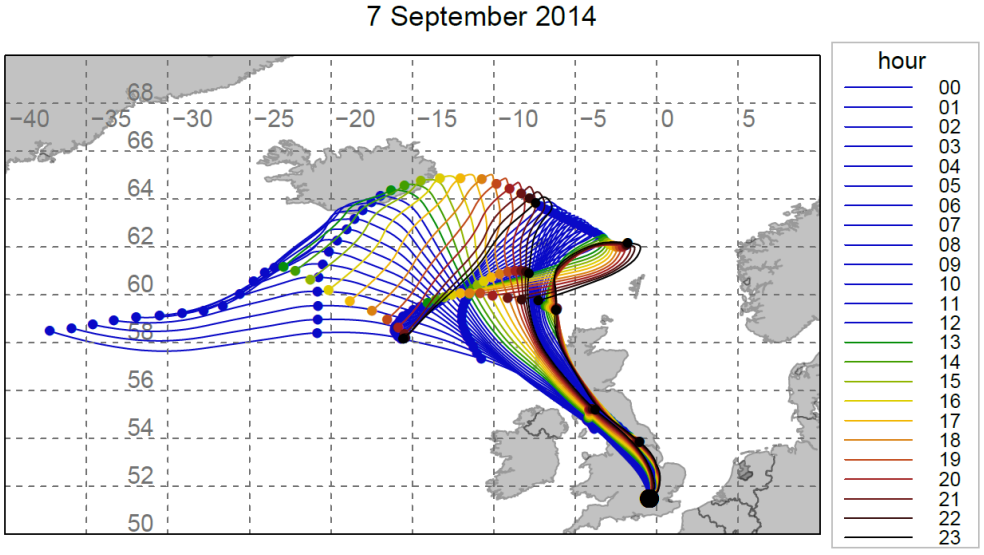

1537

1538 **Figure 11.** Backward air mass trajectories during the nucleation event. Dots indicate 24 h step times

1539

1540